

INVESTIGATION OF SILICATE MICRO-INCLUSIONS FROM ORHANELI AND HARMANCIK CHROMITITES (NW TURKEY): NEW ULTRAHIGH-PRESSURE EVIDENCE FROM WESTERN TETHYAN OPHIOLITIC CHROMITITES

Mehmet Akbulut✉

Department of Geological Engineering, Dokuz Eylül University, Izmir, Turkey.

✉ *Corresponding author, email: mehmet.akbulut@deu.edu.tr; makbulut@deu.edu.tr*

Keywords: *Ophiolitic chromitites; ultra-high pressure; deep mantle recycling; silicate lamellae in chromite; dunitic orbicular texture; Northwestern Turkey.*

ABSTRACT

In this study, mainly silicate and some sulfide micro-inclusions hosted in magnesiochromites of chromitites from Orhaneli Ophiolite Complex and Harmancik Peridotites in northwestern Turkey are studied. Existence of randomly distributed anhedral (globular), selectively oriented lamellar/needle-shaped silicate micro-inclusions and several other cubic/octahedral inclusions hosted in magnesiochromites are noted along with Ir-group platinum-group element (IPGE) bearing phases and base metal sulfides (BMS). The microscopic observations, Raman, electron dispersive and wavelength dispersive spectrometry data have shown that the randomly distributed anhedral (globular) silicate inclusions mainly consist of forsterite and diopside. Selectively oriented lamellar/needle-shaped silicate micro-inclusions are determined as diopsides. Some of the cubic/octahedral inclusions are identified as (cubic) Mg-silicates, while some other inclusions are identified as euhedral to subhedral clinopyroxene and Na-K-Ca and Mg bearing silicates. An important amount of the studied cubic/octahedral inclusions are identified as negative crystals of cubic/octahedral form (some in form of trigonal or macle crystals). The oriented lamellae/needles of diopside are found both in the Orhaneli and Harmancik chromitites. Cubic/octahedral Mg-silicates and negative crystals are only detected in a multi-textured chromitite sample (with dunitic-orbicular, semi-massive and massive textures), which lacks the oriented diopside lamellae/needles. Although no other ultra-high-pressure (UHP) phases are found, the existence of oriented diopside lamellae/needles in the Orhaneli and Harmancik chromitites are interpreted as the first in-situ evidence of UHP conditions and possibly their deep mantle recycling history. It may be speculated that the occurrence of micro-lamellae/needles of diopside in the Orhaneli chromitites within the cumulate dunites result from entrapment of recycled relics of UHP chromitites within the upwelling primordial melts that replenished the evolved magmas ponding in the MTZ. A step-by-step textural interpretation of the multi-textured Harmancik chromitite sample also suggested at least two stages of chromite formation, the former represented with the tightly packed nodular chromite nuclei within the dunitic orbicules, and the latter with surrounding semi-massive to massive (tightly packed) chromitites. The former stage can clearly be traced to be finally incorporated within the latter. The cubic/octahedral Mg-silicates and negative crystals are both seen within the first stage chromitite nuclei of the dunitic orbicules and the second stage surrounding chromitite. Occurrences of these inclusions are also questioned for a possible link between the textural evolution of chromitite and the UHP processes, and possibilities for finding a field (macroscopic) evidence for discriminating UHP chromitites. Due to some conflicting findings, it is concluded that more data are needed for reaching a final decision.

INTRODUCTION

Formation of the ophiolitic (a.k.a. podiform) chromitites has long been a matter of debate for being one of the main sources of chromium and providing first-hand valuable information on mantle events and processes (e.g., Arai and Miura, 2016). The ophiolitic chromitites mainly occur: (1) along the crust-mantle boundary (the petrographic Moho) as banded-layered chromitites within the lowermost transition dunites at the base of the crustal cumulates, or (2) as conformable/unconformable bodies concordant, subconcordant or discordant with the internal plastic deformation structures of the surrounding peridotites (tectonite peridotites) along the subjacent uppermost part of the mantle (vertically down to ~ 1 km below the petrographic Moho). Their host rocks are either dunites or harzburgites. When the host rocks are harzburgites, the chromitite bodies are always surrounded by a dunite envelope of replacive origin. Various modes of occurrences and settings had been previously discussed by several authors in detail (Thayer, 1969; Ulmer, 1969; Dickey, 1975; Juteau, 1975; Irvine 1975; 1977; Greenbaum, 1977; Brown, 1980; Johan and Le Bel, 1980; Cassard et al., 1981; Lago et al., 1982; Maurel and Maurel, 1982; Johan et al., 1983; Berger and Vannier, 1984; Ceuleneer and Nicolas, 1985; Johan, 1986; Nicolas, 1986; Kelemen, 1989; Roeder and Reynolds, 1991; Leblanc and Ceuleneer, 1992; Leblanc

and Nicolas, 1992; Arai and Yurimoto, 1994; 1995; Arai and Matsukage, 1996; 1998; Zhou et al., 1994; Rollinson and Adetunji, 2013; 2015; González-Jiménez et al., 2014; Arai and Miura, 2015; 2016).

The cumulate dunites in the Moho Transition Zone have been either suggested to be the first ultramafic cumulates of the crustal magmatic section (Jackson et al., 1975; Elthon et al, 1982) or refractory mantle residues (Sinton, 1977; Nicolas and Prinzhofer, 1983), a zone of residual mantle peridotites traversed and impregnated by ascending partial melts originated from the upper mantle (Leblanc and Nicolas, 1992). The banded-layered chromitites within the transition zone have also been largely interpreted as igneous cumulates like their host rocks and well-explained by the model of Irvine (1978) (Leblanc and Nicolas, 1992). However occurrence of chromitite pods within the tectonite peridotites well below the cumulate dunites remained as a conundrum and subject of debate (Thayer, 1969; Boudier and Nicolas, 1972; Dickey, 1975; Juteau, 1975; Greenbaum, 1977; Brown, 1980; Cassard et al., 1981; Lago et al., 1982; Nicolas, 1989; Leblanc and Nicolas, 1992). Today, latter chromitites are mostly interpreted to be formed by the reaction of mantle derived olivine-chromite saturated melts and surrounding peridotites along small melt conduits or interconnected 3-dimensional networks of film-like channels in the uppermost mantle (Lago et al., 1982; Arai and Yurimoto,

1994; Zhou et al., 1994; González-Jiménez et al., 2014; Arai and Miura, 2016). The chromitite pods in the tectonites may be concordant, subconcordant or discordant with the structural elements (e.g., primary banding and/or foliation) of their host rocks, and this alignment is affiliated with the syn- to post-formational plastic deformation processes and/or later magmatic events (cf. Cassard et al., 1981).

The magma/wall-rock reaction involving incongruent melting of the orthopyroxenes of the surrounding peridotites around the melt channel(s) is considered to be the main driving process for the formation of the reactive dunite envelopes around the ophiolitic chromitites. The discussion on the possible tectonomagmatic settings for such melt/rock interaction is still ongoing. However, both compressional (e.g., along the supra-subduction zone - SSZ fore-arc and/or back-arc settings), and extensional stress regimes (e.g., along the mid-ocean ridges - MOR settings) are favourable locations for the introduction of olivine oversaturated and pyroxene undersaturated melts, which generate the conduits into the moderately depleted peridotites enabling the formation of podiform (a.k.a., ophiolitic) chromitites (cf. Arai and Miura, 2015 and references therein). Chemical, spatial and temporal evidences suggest that the coexistence of podiform chromitites from different tectonic settings (i.e., mid-ocean ridge or forearc/back-arc) is commonly observed in several ophiolitic terranes implying a multi-episode chromitite formation process (Boudier et al., 1982; Ahmed and Arai, 2002; Arai et al., 2006; Miura et al., 2012; Uysal et al., 2012; Akbulut et al., 2016; Arai and Miura, 2016).

Recent studies performed on ophiolitic chromitites and peridotites of the eastern segment of the Alpine Himalayan Orogenic Belt (e.g., Luobusa ophiolite in southern Tibet, Sartohay ophiolite in Xinjiang, and Hegenshan ophiolite in Inner Mongolia; cf. Xu et al., 2009; 2015; Yang et al., 2014; 2015a; Huang et al., 2015; Tian et al., 2015) and Paleozoic Polar Ural orogenic belt (Yang et al., 2015b), report the existence of diamond inclusions in chromitites suggesting ultra-high pressure (UHP) and deep mantle conditions (> 150 km). These findings highly contrast with the shallow depth and low pressure genesis generally pronounced for the typical ophiolitic chromitites, due to their abundance within the petrographical Moho and/or the underlying uppermost mantle sections of well-exposed ophiolites (Arai and Miura 2016 and references therein; crust-mantle boundary corresponding up to ~ 40 km depth and ~ 1 GPa pressure; cf. Dziewonski and Anderson, 1981; O'Reilly and Griffin, 2013). The presence of several other UHP and highly reduced minerals (e.g., coesite, Ni-Mn-Co alloys, spessartite, tephroite, native elements, moissanite, Fe-Si and Fe-C phases) and/or peculiar silicate lamellae (e.g., diopside, coesite and enstatite) encountered within some chromitites from Luobusa ophiolite further suggested inversion of these current chromites from a high-pressure chromian spinel polymorph that may incorporate Ca and Si (e.g., Ca-ferrite, CF-type; CaFe_2O_4 , which is stable over 12.5 GPa and deeper than 380 km, cf. Satsukawa et al., 2015 and references therein). These data suggest effects of deeper, near Mantle Transition Zone conditions (410-660 km) for at least some part of the history of these ophiolitic chromitites (Yang et al., 2007; 2015a; Yamamoto et al., 2009; Satsukawa et al., 2015; Griffin et al., 2016). The conversion from deeper to shallower mantle environment conditions is further supported with the existence of pyroxene + spinel symplectites from some other diamond-bearing Tibetan peridotites (e.g., Hebert et al., 2003; Xiong, 2015) that are interpreted to represent breakdown of high-pressure

majoritic garnet (Griffin et al., 2016). As these deep mantle relicts are also accompanied by evidences of shallow mantle conditions, a deep mantle recycling process is suggested for these peculiar ophiolitic chromitites and peridotites (cf. Arai, 2013; Arai and Miura, 2016; Griffin et al., 2016).

Turkey is located at the western segment of the Alpine-Himalayan Belt where many fragments of the Tethyan ophiolites including numerous ophiolitic chromitite occurrences crop out. Recent studies including advanced mineral separation works have already reported several unusual crustal (e.g., zircon, monazite; Akbulut et al., 2016; Lian et al., 2017) and ultra-high pressure (UHP) phases (e.g., micro-diamonds, moissanite; Lian et al., 2017) in the southern ophiolitic massifs of the Anatolide Tauride Block. The northern ophiolite massifs of the Anatolide Tauride Block also include similar remnants of the Tethyan mantle. The above mentioned findings from chromitites of the southern ophiolite massifs encourage a similar investigation on the northern massif chromitites. This study resulted from the preliminary work for this pursuit and reports new in-situ data from several unusual inclusions hosted by chromitites of Orhaneli Ophiolite Complex and Harmancık Peridotites in northwestern Turkey. The aim of this study is to contribute to the ongoing discussion on the occurrence of UHP chromitites and the genesis of the Tethyan ophiolitic chromitites by introducing and interpreting these new in-situ findings.

GEOLOGICAL SETTING AND THE ORHANELI AND HARMANCIK CHROMITE DEPOSITS

The Alpine-Himalayan Belt (a.k.a. the Tethyan Metallogenic Belt), extending westwards to the Alps and eastwards to Tibet, is a well-known major orogenic (and metallogenic) belt which includes a set of tectonic sutures marking the closure of the several overlapping phases of the Tethyan oceans. Present day Turkey is located at the western part of this belt and its geological structure is heavily related to the dynamics of these Tethyan oceans (Fig. 1a). These dynamic processes have brought along a collage of microcontinents and a very fertile metallogenic environment, enabling observation of different continental-oceanic crustal and mantle relicts and mineralizations. These mineralizations are related to various geological epochs (ranging from Paleozoic to Cenozoic) and metallogenic provinces, along the west-east elongated tectonic belts of Turkey (Fig. 1b). These tectonic belts and related suture zones comprise several ophiolitic complexes that include remnants of Tethyan oceanic -and their predecessor subcontinental- lithospheric mantle (cf. Akbulut et al., 2016 and references therein). Two of these complexes located at northwestern Turkey are the Orhaneli Ophiolite Complex and the Harmancık Peridotites, which comprise the western segment of the "Bursa-Kütahya-Eskişehir Chromium Region", one of the six well-known and explored/exploited chromium belts of Turkey.

The Orhaneli Ophiolite Complex is located south of the western segment of the İzmir-Ankara-Erzincan Suture (e.g., Sarıfakıoğlu et al., 2009; Fig.1b), and constitutes the boundary between the Pontide and the Anatolide-Tauride Belts. The eastern part of the Orhaneli Ophiolite Complex has been thrust over the metamorphic units of Sakarya Zone (Creataceous blueschists and marbles) to the north, and Tavşanlı Zone (Late Triassic graywackes including Permian-Carboniferous limestone blocks) to the south (e.g., Sarıfakıoğlu et al., 2009; Figs. 1c and 2a). The Orhaneli Ophiolite

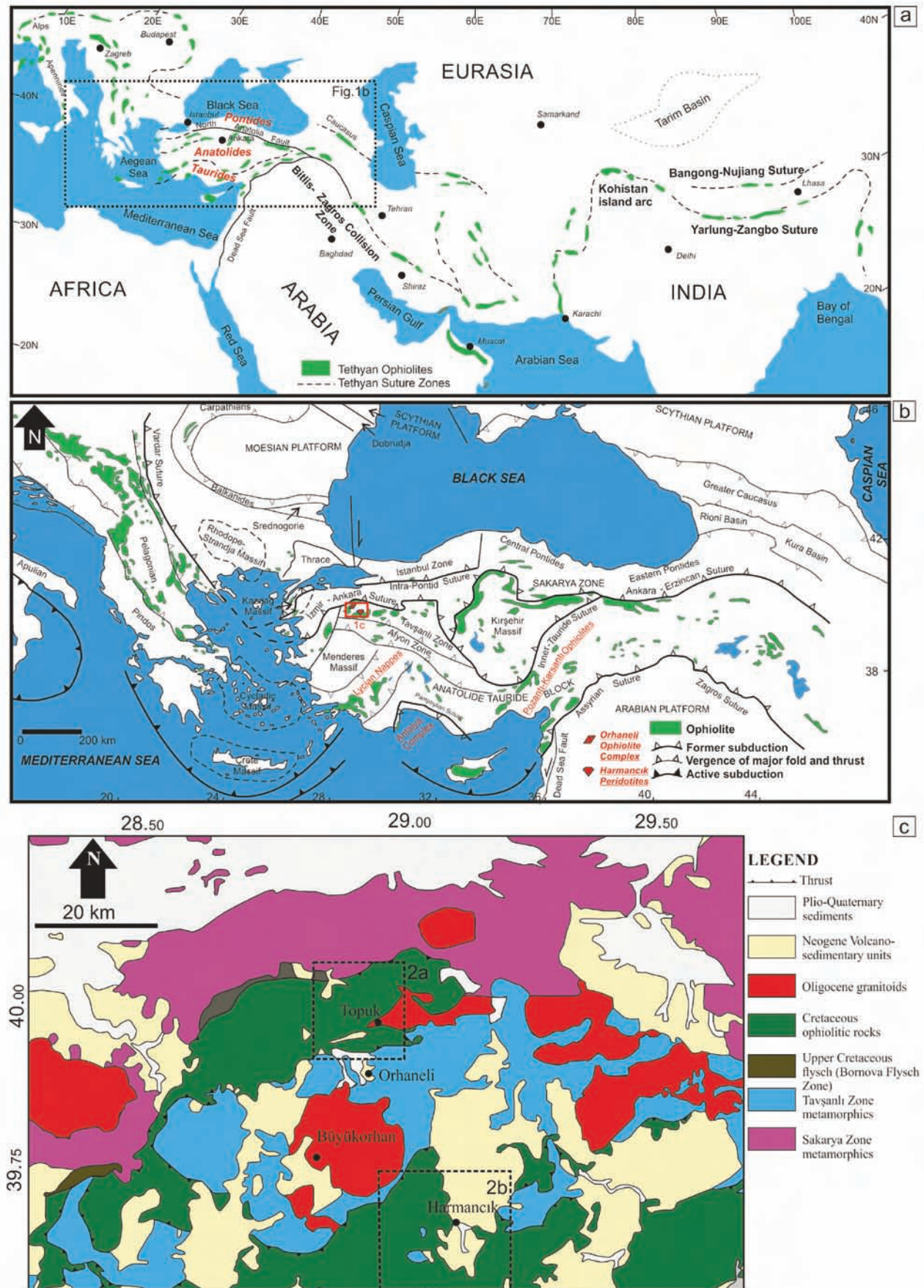


Fig. 1 - (a) Major Tethyan ophiolites along the Alpine-Himalayan Orogenic Belt (modified after Dilek and Furnes, 2009), (b) Map showing the continental blocks, major sutures and related ophiolites of the Eastern Mediterranean region (modified after Tavlan et al., 2011 and references therein). The distribution of the Crete, Cycladic, Rhodope-Strandja and Kazdağ Massifs is from Catlos and Çemen (2005). (c) The simplified geology of the Orhanlı and Harmancık Area (after MTA, 2002; Uysal et al., 2015). The location of Fig. 2 is indicated.

Complex includes relicts of an ancient mantle-crust transition zone (i.e., petrographic MOHO) comprising mainly basal ultramafic cumulates (dominated by chromitite inter-layered dunites, followed by wehrlites, lherzolites, harzburgites and pyroxenites) and to a lesser extent mafic cumulates (cumulate gabbros and gabbro-norites; e.g., Sarıfakıoğlu et al., 2009; Uysal et al., 2015; Fig. 2a). The mafic-ultramafic cumulate units present a repetitive cycling and the ultramafic cumulates are locally cut by isolated diabase dykes (e.g., Sarıfakıoğlu et al., 2009). The Eocene Topuk granodiorite cuts both the metamorphic autochthonous units and the overthrusting Orhaneli Ophiolite Complex (e.g., Harris et al., 1994; Sarıfakıoğlu et al., 2009).

The Harmancık Peridotites are located to the southeast of the Orhaneli Ophiolite Complex (Fig. 1c). The Harmancık Peridotites are covered to the east by Neogene volcano-sedimentary units (lacustrine basal conglomerates and coarse-grained sandstones including coal layers) (e.g., Uysal et al., 2014; 2015). They are thick slabs thrust onto the metamorphic Tavşanlı Zone (Paleozoic blueschists and recrystallized carbonate rocks) to the northwest of Harmancık (Fig. 1c; Uysal et al., 2015). The crystalline basement is cut by a granitic intrusion to the northwest (Borchert and Uzkut, 1967). The Harmancık Peridotites are mainly composed of moderately to strongly serpentinized harzburgites and dunite tectonite intercalations (Fig. 2b).

The chromitite interlayers within the dunites of the Orhaneli Ophiolite Complex cumulate sequence are a major source of economic interest. Several of these chromitite occurrences are utilized as chromite deposits and exploited for chromium, while the accompanying huge dunite masses are also sometimes exploited for olivine. These chromitite interlayers occur as a result of rhythmic layering of chromite and olivine cumulus crystals, presenting massive to semi-massive banded (a.k.a. stratiform, cumulate) chromitite structure (Fig. 3a-c), usually with a low grade ore character (< 30%, cf. Gültaşlı, 1996). The thickness of the chromitite bands typically ranges between 0.5 and 5 cm, rarely reaching up to ca. 10 cm. Thinner bands (or trails) of chromite may present agglomerations that form small lenticular chromitite schlierens that are concordant with the thicker chromitite bands (Fig. 3c-g).

The chromitites within the Harmancık Peridotites tectonites are also of major economic importance. They are always found as cm to meters scale orebodies included in thick dunite intercalations within the harzburgites (Fig. 4a). Lenticular/tabular chromitite pods and schlierens/bands are common (Fig. 4b and c). They usually present typical massive to semi-massive, disseminated, nodular, and rarely orbicular textures (Fig. 4d), with the nodules sometimes elongated along the strike of the chromitite bands (Fig. 4e). One notable sample (sample 71), obtained from the active mining site located northwest of Harmancık, distinctly presents a multi-textured appearance including rare dunitic orbicular, semi-massive and massive textures (Fig. 4f-j). The dunitic orbicular texture is characterized by usually spherical chromitite nuclei surrounded by spherical to elliptical dunitic shells, further enclosed by a second phase of chromite agglomeration grading into semi-massive to massive chromitite (Fig. 4h-j).

SAMPLING AND ANALYTICAL PROCEDURES

Several active and abandoned chromite deposits from the eastern segment of the Orhaneli Ophiolite Complex and

Harmancık Peridotites were sampled in this study (Fig. 2a and b). Sampling from the chromitites was mostly done by random picking of chromitite bands and schlierens, from the chromitite stockpiles-wastes at the active/abandoned mine sites and/or outcrops where available (Figs. 3 and 4). The multi-textured sample described above (sample 71, Fig. 2b and 4f-j) was provided by company officials from the active mining site of CVK Group (CVK Mineral ve Madencilik A.Ş.) from the Harmancık (Bursa, Turkey) chromium operation.

The chromitite samples were impregnated in epoxy resin and carefully polished for petrography, mineral chemistry and Laser-Raman spectroscopy at the Fluid Inclusion and Ore Microscopy-Petrography Laboratory of Geological Engineering Department of Dokuz Eylül University (DEU, Izmir, Turkey). Studies under the reflected light are also completed in this facility with Leica DM2500P and Nikon E400POL microscopes. Back-scattered electron (BSE) images and EDS (Energy-Dispersive X-ray Spectroscopy) analyses of the selected chromitite grains, platinum-group minerals (PGM), base-metal sulfides (BMS), silicate and other unusual inclusions in chromitites were obtained using three Scanning Electron Microscopes (SEM) at: (1) Center for Material Research of Izmir Institute of Technology (IZTECH, FEI Quanta 250 FEG SEM), (2) Central Laboratory of Middle East Technical University (METU, Quanta 400F Field Emission SEM), and (3) Central Research Laboratory of Izmir Katip Çelebi University (IKCU, Carl Zeiss 300VP SEM). X-ray mapping studies are completed at METU and IKCU facilities.

Several of the detected silicate micro-inclusions were analyzed with a JEOL JXA-8230 electron probe micro-analyzer (EPMA) at the Central Laboratory of METU. Analytical conditions were 15kV acceleration voltage, 15 nA beam current and spot size ($\geq 1 \mu$) beam diameter. The standards used were albite for Na, wollastonite for Si and Ca, Al_2O_3 , MgO, Fe_2O_3 , TiO_2 and Cr_2O_3 for Al, Mg, Fe, Ti and Cr, respectively, Ni-metal for Ni, rhodonite for Mn, and orthoclase for K.

Laser-Raman spectroscopy studies on the silicates and other micro-inclusions were completed by a Confocal Renishaw inVia Raman Microscope and Spectrometer installed at the Central Research Laboratory of IKCU. All the spectra reported in this study were acquired with 532 nm excitation, 2400 line/mm grating and under 20x to 100x optical zoom. Removal of background and peaks related to cosmic-ray events (CRE) was done by CrystalSleuth Raman Spectroscopy software (Laetsch and Downs, 2006). Evaluation of the obtained spectra was completed by comparing/matching the obtained spectra with the Raman spectra library of RRUFF database (<http://rruff.info>) embedded within the CrystalSleuth Raman Spectroscopy software. The RRUFF ID-numbers of the reference spectra used for comparison are given in the related figures.

PETROGRAPHY AND GEOCHEMISTRY OF THE CHROMITE AND MINERAL INCLUSIONS IN THE CHROMITITES

Chromite

The chromitites from the Orhaneli Ophiolite Complex generally present adcumulus- to orthocumulus-like texture with subhedral to anhedral -usually fresh- chromite grains (with minor ferrite-chromite occurrences along the cracks of

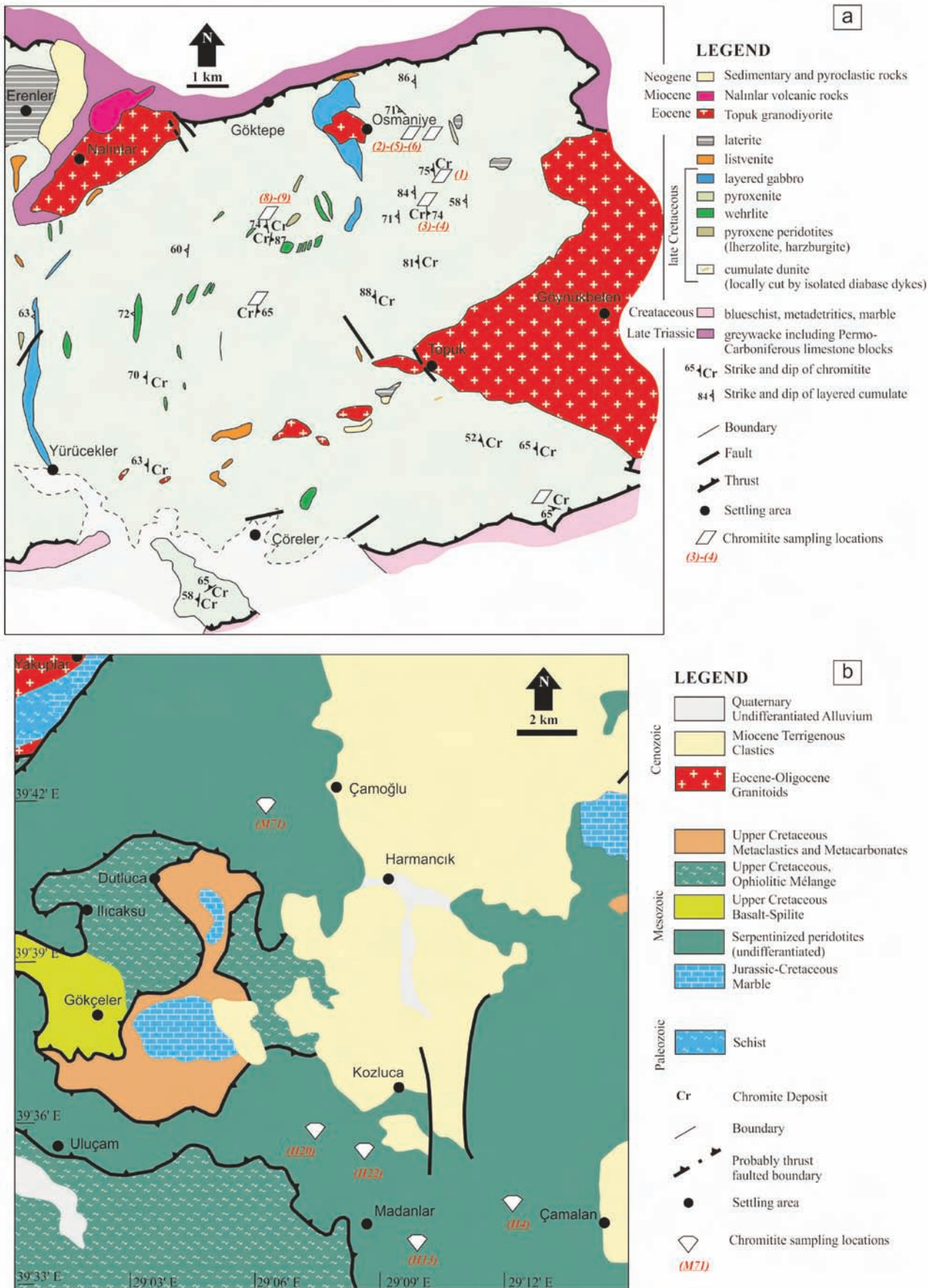


Fig. 2 - (a) Detailed geological map of the eastern segment of the Orhaneli Ophiolitic Complex (after Özen et al., 2004; Sarfakıoğlu et al., 2009) and sampling localities. (b) Geological map of Harmancık and surroundings, and sampling locations (established using Geoscience Map Viewer and Drawing Editor of General Directorate of Mineral Research and Exploration -MTA- that utilize geological map of Turkey compilation by Akbaş et al., 2001). For the location of these maps see Fig. 1.



Fig. 3 - Field and sample photos from Orhaneli chromitites. (a) - (c) Banded chromitites that occur by rhythmic layering of chromitite (Chromitite- Cr) and olivine cumulus crystals (Dunite-Du). (c) - (e) Thinner bands (or trails) of chromitite agglomerating to form small lenticular chromitite schlierens concordant/semiconcordant with the thicker chromitite bands. (f) and (g) Thicker bands of chromitite from Orhaneli region. Fig. 3e is after Fidan (2016). Fig. 3e - g shows the banded chromitite samples that include lamellar/needle-shaped silicate micro-inclusions.

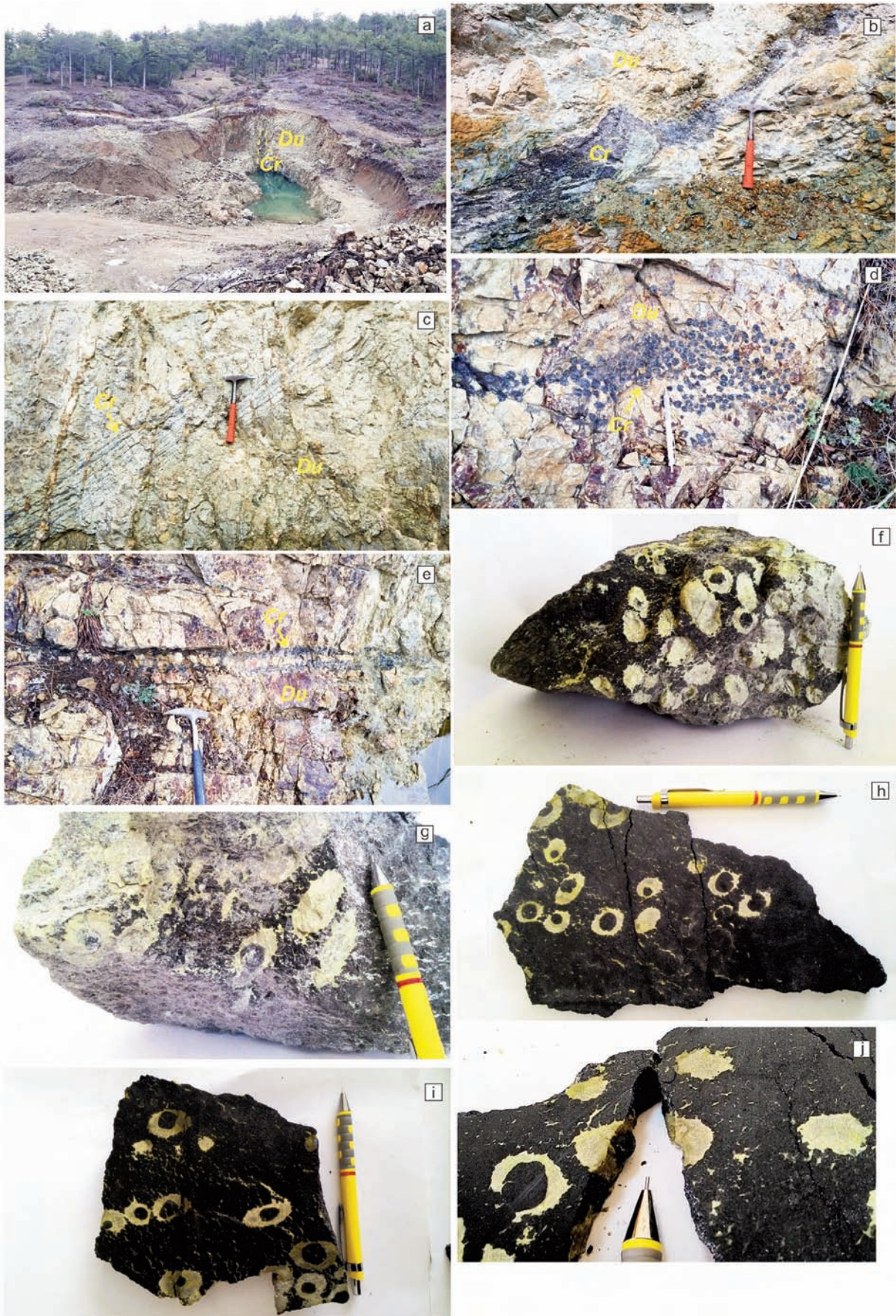


Fig. 4 - Field and sample photos from Harmancik chromitites. (a) General view of an abandoned chromite mining site; the chromitite-dunite contact is marked with yellow dashed lines (Chromitite- Cr, Dunite- Du). (b) and (c) Lenticular chromitite schlierens/bands in dunite. (d) and (e) Spherical and elongated nodular chromites in dunite. (f) to (j) The multi-textured chromitite sample from the active chromite mining site of CVK Group's (CVK Mineral ve Madencilik A.Ş.) Harmancik (Bursa, Turkey) operation.

the chromites) agglomerating to form larger chromite crystals and leading to the formation of chromitite bands and schlierens in the cumulate dunites (Fig. 3). The intercumulus/interstitial phases are generally serpentinized olivine. In contrast, chromitites from the Harmancık Peridotites show massive, semi-massive, disseminated, nodular and/or orbicular textures (Fig. 4b-e), with interstitial silicate matrix usually made of partially or totally serpentinized olivine. Some samples may also include pyroxenes and amphiboles in their matrix. The elongated nodules sometimes present typical extensional pull-apart structures oriented nearly perpendicular to the axis of elongation. The individual chromite grains are mostly subhedral to anhedral, agglomerating to form larger chromite grains and present minor ferrite-chromite occurrences along the cracks. These chromite agglomerations/accumulations form lenticular/tabular chromitite pods and occasionally the schlierens/bands in the thick and heavily serpentinized dunitic intercalations within the porphyroclastic textured harzburgitic tectonite peridotites. Cataclastic texture is common in shear zones of chromitites from both regions.

The multi-textured sample from Harmancık Peridotites (Fig. 4f-j), with semi-massive to massive chromitites enclosing dunitic orbicules with chromitite nuclei, shows distinct characteristics that must be noted. (1) The tightly packed chromitite core nodules occur within dunitite that is almost free of chromite (almost solely made of serpentinized olivine), possibly via agglomeration of smaller chromite grains. (2) The sizes of the chromite cores and their dunitic shells are usually unrelated and dunitite nodules in similar sizes may contain chromitite cores with different sizes. (3) The dunitic shells are aligned and elongated and/or flattened along an axis (as also usually seen in resembling typical anti-nodular textures elsewhere, Fig. 4f and g). (4) The enclosing semi-massive to massive chromitites seem to imitate some sort of chromite “crystal rain” pouring over the dunitic shells (probably also assisting the elongation or flattening of these shells). (5) Although the elongation/flattening of the dunitic shells does not primarily seem to affect their chromitite cores, the progressive chromite crystallization and crystal rain seems to flatten and shrink the dunitic shells to an extent that the core chromitites are squeezed towards the walls of their dunitic shells, finally losing their structural integrity and incorporating with the enclosing intensive chromite crystallization (middle right of the Fig. 4h). (6) Finally, the chromite crystallization and crystal rain ends up forming a very tightly packed massive chromitite envelope (almost free of interstitial silicates, right of the Fig. 4h).

The major-element composition of chromite grains from the chromitites of Orhaneli Ophiolite Complex and Harmancık Peridotites has previously been discussed by Uysal et al. (2015) who reported that these chromitites consist of “magnesiocromites” with usually typical high-Cr character ($Cr\#$ [$Cr/(Cr+Al)$ atomic ratio] between 0.80 and 0.83 and $Mg\#$ [$Mg/(Mg+Fe^{2+})$ atomic ratio] between 0.52 and 0.69) and boninitic affinity (with low TiO_2 values *ca.* < 0.20 wt%). Uysal et al. (2015) further noted that one sample from their Orhaneli Ophiolite Complex dataset differs from the others with relatively lower $Cr\#$ (0.68 in average) and higher TiO_2 content (up to 0.30 wt%) and resembles to the magnesiocromites of island arc tholeiite (IAT) affinity rather than to that of the boninites, suggesting a polygenetic arc-related (e.g., subduction related) environment for the tectonic setting of Orhaneli and Harmancık chromitites.

Platinum-Group Mineral and Base Metal Sulfides

A detailed discussion of the BMS and PGM phases in Orhaneli and Harmancık chromitites are also given in Uysal et al. (2015). Our new supplementary observations of the PGM and BMS from these chromitites are in good agreement with this previous study. The new observations show that the chromite and intercumulus/interstitial silicates of Orhaneli and Harmancık chromitites include scarce PGM and BMS, the former generally as mono- and rarely poly-phase inclusions in chromites. The BMS are generally found at the chromite-intercumulus/interstitial phase boundaries, chromite cracks and/or directly within these intercumulus/interstitial silicate phases. Rarely, they may also occur as mono- or polyphase inclusions in chromites. The detected PGM phases from Orhaneli chromitites consist of Ir- and mostly Os-bearing laurite end-members of the laurite-erlichmanite series (Fig. 5a). Only a single irarsite is detected. The grain sizes of these PGMs approximately range between 2 to 20 μm . The BMS phases determined are pentlandite, violarite, heazlewoodite, millerite, pyrite and awaruite. The PGM phases detected from the Harmancık chromitites are also similar with the ones from the Orhaneli chromitites and consist of Ir-, As- and Os-bearing laurites (Fig. 5b). The BMS species are rather less abundant than the Orhaneli chromitites and the detected ones are determined as heazlewoodite and pyrite. The grain sizes of the PGMs found are inbetween 4 to 5 μm .

Silicates

Globular/anhedral silicate inclusions are ubiquitous in chromites from both the Orhaneli Ophiolite Complex and the Harmancık Peridotites. The studied ones are determined as forsterite and diopside (Fig. 5c and d, Table 1 and 2), and forsterite, in Orhaneli and Harmancık chromitites respectively (Fig. 5e and f). Besides these globular/anhedral silicate inclusions, some rare chromite grains in both Orhaneli and Harmancık chromitites have minute lamellar or needle-shaped silicate micro-inclusions (usually < 50 μ in length and < 1 μ in width, Fig. 5g-o). The depth profile (or height) of these inclusions are unknown thus, these may either be interpreted as micro-lamellae and/or micro-needles. Unlike the globular/anhedral silicate inclusions, these lamellar/needle-shaped inclusions are not randomly distributed and instead appear to follow certain (preferred?) crystallographic orientations (Fig. 6a and b). At least three sets of these orientated inclusions are found to be intersecting at angles between *ca.* 54 and 68° (Fig. 6b and c). Rarely, the lamellar/needle-shaped inclusions seems to overgrow on the globular diopside inclusions (Fig. 6d).

The X-Ray elemental mapping completed in some of these occurrences has shown that the micro-lamellae and/or needles are characterized by the significant presence of Si and Ca (Fig. 7a-c, i-k) and absence of Cr, Al and Fe (Fig. 7a, e-g, i, m-o). Changes in Mg and O contents are very small, almost negligible (Fig. 7a, d, h, i, l and p). Electron Dispersive Spectrometry (EDS) and Wavelength Dispersive Spectrometry (WDS) studies completed in some relatively larger lamellar/needle-shaped micro-inclusions (Table 1 and 2) show somewhat mixed elemental abundances, probably largely due to the insufficient thickness and depths of these inclusions (smaller than the beam spot size, < 1 μ). The obtained data are notably characterized by important addition of Cr, probably from the host chromitite. However, the data also show significant amounts of Ca and Si, compatible with the X-Ray elemental mapping data.

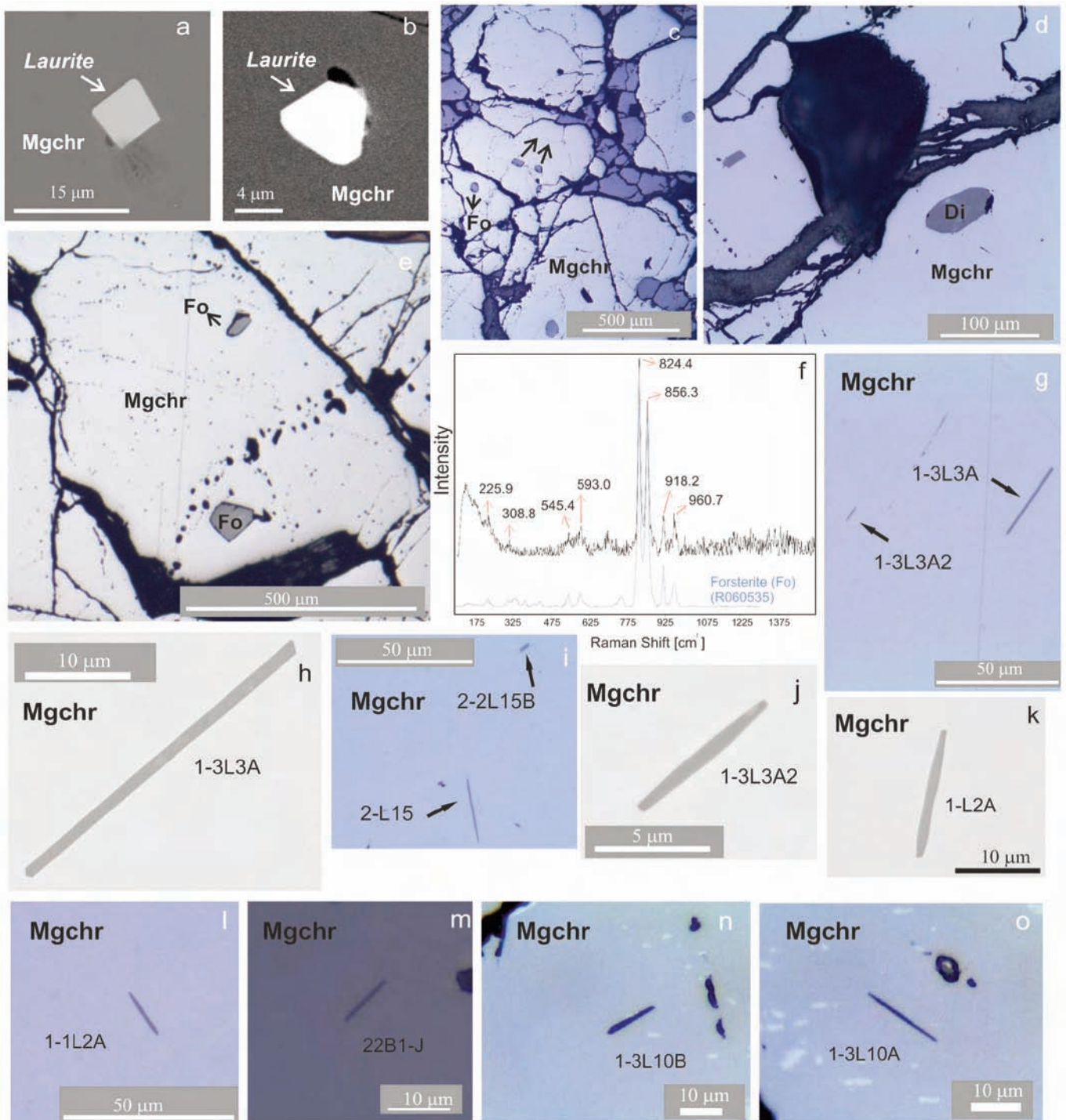


Fig. 5 - (a) and (b) BSE images of laurite inclusions detected in the magnesiochromites (Mgchr) of the Orhaneli and Harmancik chromitites. (c)-(e) Randomly distributed globular/anhydral forsterite (Fo) and diopside (Di) inclusions in the magnesiochromites of the Orhaneli and Harmancik chromitites. (f) Raman spectrum of a globular/anhydral forsterite from Harmancik chromitites. The reference spectra used for comparison of forsterite peaks is shown with blue coloured line together with its RRUF ID-number (<http://rruff.info>). (g), to (o) Minute lamellar/needle-shaped silicate micro-inclusions detected in some of the magnesiochromites of the Orhaneli and Harmancik chromitites.

As the width of almost all of the silicate micro-lamellae and/or needles are usually $< 1 \mu\text{m}$, and rarely $> 50 \mu\text{m}$ in length, all of the obtained raman spectra from the lamellar/needle shaped inclusions encountered in Orhaneli and Harmancik chromitites also show somewhat composite Raman spectra, including peaks from diopside and their host magnesiochromite grains (Fig. 8a-h). However, careful evaluation of these composite spectra has revealed certain characteristic bands that may correspond to the M-O stretching (at

$ca. 327 \text{ cm}^{-1}$), Mg-O stretching (at $ca. 393 \text{ cm}^{-1}$), Si-O-Si bending (at $ca. 665 \text{ cm}^{-1}$) and Si-O^(br) stretching (at $ca. 1010 \text{ cm}^{-1}$) modes of diopside (Fig. 8a-h; cf. Huang et al., 2000). In larger (thicker) micro-lamellae, additional bands of Ca-O stretching (at $ca. 360 \text{ cm}^{-1}$) and Si-O^(br) stretching (at $ca. 853 \text{ cm}^{-1}$ and $ca. 1047 \text{ cm}^{-1}$) modes of diopside may also be observed (Fig. 8h; cf. Huang et al., 2000). This is in good agreement with their Si, Ca and O bearing, and Cr, Al and Fe deficient chemistry described above. Thus, these rare

Table 1 - Selected electron dispersive spectrometry (EDS) data from the globular/anhydral and lamellar/needle shaped micro inclusions in magnesiochromites of the Orhaneli and Harmancik chromitites.

Wt. %*	Lamellar/ needle shaped Inclusions																
	Globular/ anhydral Inclusions		Dioptside														
	I-1JLA	22A51A1	I-3L2A	I-3L2B	I-3L3A	I-3L3A2	I-3L4A	I-3L4B	I-3L4C	I-3L5A	I-3L5B	I-3L8A	3-3L3A	3-3L8A	22B1F4	22B1F2A	22A51A2
O	41.97	32.08	38.69	38.16	40.24	38.87	37.70	37.98	39.06	39.59	37.46	37.64	38.80	36.01	20.16	19.74	29.24
Mg	11.09	13.76	9.83	9.52	10.13	9.62	8.94	9.32	9.54	10.04	9.69	9.15	9.79	9.40	12.69	10.88	12.96
Al	1.17	6.67	2.54	2.89	1.92	2.47	3.01	2.84	2.37	2.30	3.02	3.15	2.37	3.33	6.03	5.84	6.35
Si	20.66	18.81	13.61	12.42	17.06	14.15	11.68	12.22	14.56	15.48	10.86	11.47	13.62	7.36	13.65	10.65	17.19
Ca	12.05	6.72	8.62	8.11	10.35	8.66	8.03	7.45	9.93	9.67	6.09	7.60	9.95	4.13	4.56	6.93	6.80
Cr	8.80	16.20	19.26	20.87	14.20	18.59	22.03	21.59	17.65	16.41	23.86	21.94	19.76	31.03	32.73	35.03	20.33
Fe	4.27	5.75	7.46	8.03	6.10	7.63	8.61	8.61	6.89	6.51	9.01	9.06	5.71	8.74	10.17	10.92	7.13
Total	100.00	99.99	100.00	100.00	100.00	100.00	100.00	100.00	100.00	100.00	100.00	100.00	100.00	100.00	99.99	99.99	100.00
Atomic %*																	
O	59.56	49.26	58.70	58.55	59.17	58.81	58.48	58.58	58.82	58.95	58.38	58.41	58.70	58.02	36.88	37.17	46.90
Mg	10.35	13.91	9.81	9.61	9.80	9.58	9.12	9.46	9.45	9.84	9.94	9.34	9.75	9.97	15.27	13.48	13.68
Al	0.98	6.08	2.28	2.63	1.68	2.22	2.77	2.60	2.12	2.03	2.79	2.90	2.13	3.18	6.54	6.52	6.04
Si	16.71	16.45	11.76	10.86	14.29	12.19	10.32	10.73	12.49	13.13	9.64	10.14	11.74	6.76	14.22	11.43	15.71
Ca	6.83	4.12	5.22	4.97	6.07	5.23	4.97	4.59	5.97	5.75	3.79	4.71	6.01	2.66	3.33	5.21	4.35
Cr	3.84	7.65	8.99	9.85	6.42	8.65	10.52	10.24	8.18	7.52	11.44	10.47	9.20	15.38	18.42	20.30	10.04
Fe	1.73	2.53	3.24	3.53	2.57	3.31	3.82	3.80	2.97	2.78	4.02	4.03	2.47	4.03	5.33	5.89	3.27
Total	100.00	100.00	100.00	100.00	100.00	100.00	100.00	100.00	100.00	100.00	100.00	100.00	100.00	100.00	99.99	100.00	99.99
Oxide %*																	
MgO	18.38	-	16.29	15.78	16.80	15.96	14.82	15.45	15.82	16.65	16.07	15.17	16.23	15.58	-	-	-
Al₂O₃	2.20	-	4.80	5.46	3.63	4.67	5.68	5.36	4.49	4.35	5.71	5.96	4.49	6.29	-	-	-
SiO₂	44.21	-	29.11	26.58	36.49	30.26	24.99	26.13	31.15	33.11	23.23	24.54	29.13	15.75	-	-	-
CaO	16.86	-	12.07	11.35	14.48	12.12	11.23	10.43	13.89	13.53	8.52	10.63	13.92	5.78	-	-	-
Cr₂O₃	12.86	-	28.15	30.51	20.75	27.17	32.20	31.55	25.80	23.99	34.88	32.06	28.88	45.35	-	-	-
FeO	5.49	-	9.59	10.33	7.85	9.82	11.07	11.07	8.86	8.37	11.59	11.65	7.34	11.24	-	-	-
Total	100.00	-	100.00	100.00	100.00	100.00	100.00	100.00	100.00	100.00	100.00	100.00	100.00	100.00	-	-	-

*: Energy Dispersive Spectrometry (EDS) data.

Table 2 - Selected wavelength dispersive spectrometry (WDS) data from the globular/anhydral and lamellar/needle shaped micro inclusions in magnesiocromites of the Orhaneli chromitites.

Wt. %*	Lamellar/ needle shaped Inclusions															
	Globular/ anhydral Inclusions							Lamellar/ needle shaped Inclusions								
	Forsterite 6-GLIA	Forsterite 6-GLIB	Forsterite 6-GLIC	1-3L12A	2-L15	2-2L15B	2-L23	1-3L342	1-3L8A	1-3L9A	1-3L9B	3-3L5B	4-3L4A	4-3L8A	4-3L8B	5-L6L14
SiO ₂	42.21	42.42	42.48	4.21	9.27	34.83	7.62	6.11	13.57	12.30	12.36	24.62	16.97	4.17	17.99	24.32
Al ₂ O ₃	0.03	0.01	0.00	9.21	7.61	3.26	7.95	8.64	7.56	7.68	7.68	4.91	5.73	7.87	5.23	5.18
MgO	52.01	52.40	52.05	10.91	13.34	14.44	13.03	11.08	11.74	12.03	12.39	15.29	14.03	12.96	13.62	12.91
FeO	2.60	2.31	2.33	17.96	12.86	5.45	12.42	16.81	15.03	15.71	15.71	9.28	10.40	14.40	9.79	6.11
NiO	0.68	0.60	0.56	0.09	0.04	0.06	0.13	0.06	0.09	0.11	0.07	0.07	0.07	0.14	0.09	0.09
TiO ₂	0.00	0.00	0.00	0.23	0.17	0.16	0.16	0.22	0.20	0.24	0.24	0.15	0.17	0.15	0.13	0.12
CaO	0.02	0.03	0.00	2.13	4.91	17.75	3.76	3.08	6.52	5.83	5.60	11.17	7.32	1.70	9.44	14.11
Na ₂ O	0.00	0.03	0.02	0.01	0.04	0.18	0.03	0.00	0.04	0.03	0.04	0.09	0.06	0.03	0.09	0.15
MnO	0.04	0.05	0.01	0.17	0.07	0.02	0.03	0.13	0.11	0.06	0.15	0.04	0.07	0.12	0.08	0.08
K ₂ O	0.00	0.00	0.00	0.01	0.01	0.01	0.00	0.01	0.01	0.00	0.00	0.00	0.01	0.00	0.00	0.00
Cr ₂ O ₃	0.92	0.68	0.98	50.55	49.11	22.70	50.25	50.09	43.81	44.73	45.71	34.52	42.93	56.13	40.01	40.19
Total	98.51	98.53	98.44	95.47	97.43	98.86	95.38	96.24	98.63	98.68	99.94	100.14	97.76	97.67	96.46	103.27

*: Wavelength Dispersive Spectrometry (WDS) data.

micro-inclusions in magnesiocromites of Orhaneli and Harmancık chromitites are selectively oriented diopside micro-lamellae and/or needles hosted within magnesiocromites.

The multi-textured chromitite sample from Harmancık Peridotites does not include the diopside micro-lamellae/needles described above. However, this sample presents other interesting inclusions such as “faceted” micro-inclusions and possible traces of micro-inclusions in form of negative crystals within its magnesiocromites. These micro-inclusions/negative crystals are mainly concentrated in the chromitite nuclei entrapped within the dunitic orbicules that are surrounded by the second generation of chromitite (Fig. 4f-j). Some of these are also observed within the magnesiocromites of the massive chromitite segment of the sample. The sizes of these micro-inclusions/negative crystals are almost always < 50 µm. Their concentration mostly within the chromitite nodules at the cores of the structure has given these host chromites an unusual “peppered-like” appearance (Fig. 9a). A closer-look at these inclusions shows that most of them have subhedral to euhedral shapes presenting clear triangular and cubic forms (Fig. 9b and c). When the microscope lens is slightly defocused under the reflected light, most of the cubic shaped inclusions present “octahedral” forms under crossed polars (Fig. 9c and d). Similarly, some of the triangular shaped inclusions (also sometimes with a defocused microscope lens) show facets of twinning according to spinel law, closely resembling to the “macle” crystals (Fig. 9e and f). Anhedral inclusions are also present but they are very rare (Fig. 9g).

The BSE imaging and EDS spectra from the cubic or octahedral inclusions confirm that most of these are negative crystals of cubic/octahedral shape within the host magnesiocromite (Fig. 9h, i and j; Table 3). The BSE imaging and EDS data of the remaining subhedral, euhedral or rare anhedral inclusions show that they are inclusions with various chemical compositions (Table 3). No carbon coating is applied to the polished sections during sample preparation (only Au coating is applied when needed), however one of the euhedral cubic phases presents high C and low Si contents (47.15 and 3.84 at. %, Fig. 9k; Table 3). This points to a Mg-bearing carbonate species, possibly magnesite. The minor Si content may be contributed from a coexisting silica phase, possibly serpentine. The direct relation of the analyzed area to a nearby crack crosscutting the host magnesiocromite (Fig. 9k) also supports this consideration and suggests a post-magmatic infill, possibly in one of the voids of negative cubic/octahedral crystal form discussed above.

Although the presence of Cr, Fe, and certain amounts of Mg, Al and O may be related to the interaction from the magnesiocromite host (due to the shape/depth of the electron interaction volume), the additional Na, Si, K and Ca components in some of the anhedral and/or subhedral cubic inclusions suggests the presence of Na-K-Ca and Mg bearing silicates (pargasite?, Table 3; Fig. 9g). The lack of Na and K and presence of Ca and Si components in some other euhedral and subhedral cubic to macle shaped inclusions also show the existence of euhedral/subhedral clinopyroxene (diopside?) inclusions (Table 3; Fig. 9f). The EDS data from another set of euhedral/subhedral cubic shaped inclusions show presence of Si and absence of Na, K and Ca (Table 3; Figs. 9l and m). The presence of Cr and certain amounts of Mg, Al, Fe and O may again be affiliated to the host magnesiocromites, however, the rest of the Mg, Al, Fe, O and the presence of important amounts of Si suggest that these euhedral/subhedral micro-inclusions are Mg-silicates of cubic form.

Table 3- Selected electron dispersive spectrometry (EDS) data from the cubic/octahedral negative crystals, euhedral/subhedral/anhydral Mg-silicates, clinopyroxene, Na-K-Ca and Mg bearing silicates, and magnesite infill in negative crystal.

	71D434	71D41A	71D42ZB	71D51B	71D43Y	711B4	71D42EA	71D43V	71D43Z	71D51C	71D42B	71D42EB	71D71Z	71D42Z1
Wt. %*	Nccos	Nccos	Nccos	E/C	S/C	E/M	E/C	S/C	S/C	S/C	A	S/C	S/C	MgstNccos
C	n.d.	n.d.	n.d.	0.13	n.d.	n.d.	0.01	0.01	n.d.	0.02	n.d.	n.d.	n.d.	26.88
O	10.69	12.08	9.24	30.11	19.65	27.73	26.45	26.48	22.39	22.47	24.61	26.08	23.85	17.94
Na	n.d.	n.d.	n.d.	n.d.	n.d.	n.d.	n.d.	n.d.	n.d.	n.d.	2.40	1.61	2.60	n.d.
Mg	7.04	8.19	6.34	24.58	19.80	13.86	18.39	18.90	15.45	17.70	17.18	16.23	16.39	9.55
Al	3.78	4.03	3.29	7.25	5.91	5.86	7.82	8.71	5.58	8.64	8.65	5.46	8.11	2.68
Si	0.18	0.58	0.39	15.64	10.48	19.27	17.92	17.70	15.11	17.64	15.22	19.91	13.78	5.12
K	n.d.	n.d.	n.d.	n.d.	n.d.	n.d.	n.d.	n.d.	n.d.	0.91	0.76	n.d.	1.07	n.d.
Ca	n.d.	n.d.	n.d.	n.d.	n.d.	7.29	1.96	0.50	2.09	0.58	n.d.	4.61	n.d.	n.d.
Cr	61.77	59.57	63.73	20.10	32.20	20.05	21.27	21.21	29.88	23.70	23.87	19.62	25.26	26.14
Fe	16.53	15.53	17.00	2.19	11.96	5.94	6.20	6.48	9.50	8.34	7.31	6.48	8.94	11.69
Total	99.99	99.98	99.99	100.00	100.00	100.00	100.02	99.99	100.00	100.00	100.00	100.00	100.00	100.00
Atomic %*														
C	n.d.	n.d.	n.d.	0.26	n.d.	n.d.	0.03	0.03	n.d.	0.03	n.d.	n.d.	n.d.	47.15
O	25.82	28.12	23.07	45.29	35.41	44.66	42.31	42.18	39.13	37.70	40.25	41.93	39.84	23.63
Na	n.d.	n.d.	n.d.	n.d.	n.d.	n.d.	n.d.	n.d.	n.d.	n.d.	2.73	1.80	3.02	n.d.
Mg	11.19	12.54	10.42	24.33	23.48	14.69	19.36	19.82	17.77	19.55	18.49	17.17	18.01	8.27
Al	5.41	5.57	4.87	6.47	6.32	5.60	7.42	8.23	5.78	8.60	8.39	5.21	8.03	2.10
Si	0.25	0.77	0.56	13.40	10.76	17.68	16.33	16.07	15.04	16.86	14.18	18.24	13.11	3.84
K	n.d.	n.d.	n.d.	n.d.	n.d.	n.d.	n.d.	n.d.	n.d.	0.63	0.51	n.d.	0.73	n.d.
Ca	n.d.	n.d.	n.d.	n.d.	n.d.	4.69	1.25	0.32	1.46	0.39	n.d.	2.96	n.d.	n.d.
Cr	45.90	42.65	48.94	9.30	17.86	9.93	10.47	10.40	16.07	12.23	12.01	9.71	12.98	10.60
Fe	11.44	10.35	12.15	0.94	6.18	2.74	2.84	2.96	4.76	4.01	3.43	2.99	4.28	4.41
Total	100.01	100.00	100.01	99.99	100.01	99.99	100.01	99.99	100.01	100.00	99.99	100.01	100.00	100.00

*: Energy Dispersive Spectrometry (EDS) data, Nccos: negative crystal of cubic/octahedral shape, E: euhedral, S: subhedral, A: anhydral, C: cubic, M: macle shaped, MgstNccos: magnesite infill in negative crystal of cubic/octahedral shape

A new cubic Mg-silicate (with the space group of ringwoodite but with an inverse-spinel structure) was recently described from the fractions separated from the chromitites of Yarlung-Zangbo Suture Zone (YZSZ, southern Tibet, China) and was provisionally named as the phase “BWJ” by Griffin et al. (2016). Similar mineral specie was also separated from the Pozanti-Karsanti ophiolitic chromitites (southern Turkey) by Lian et al. (2017), although these authors call these phases as “silicates of octahedral pseudomorph”. Griffin et al. (2016) also reported some faceted antigorite pseudomorphs within the YZSZ chromitites which they interpreted as hydrated (altered) versions of this cubic Mg-silicate. However, both author groups did not report any direct in-situ appearances of this phase. The morphology of the euhedral/subhedral cubic to octahedral negative crystals and the cubic Mg-silicate inclusions in the current study notable resemble to those separates reported earlier from the Tibetan and Turkish chromitites. Although the crystal data and structure refinement details are not set in this study, the limited qualitative chemical compositions obtained from the cubic Mg-silicate inclusions also resembles to those reported earlier (Table 3). Moreover, these cubic Mg-silicate inclusions coexist with analogous shaped negative crystals that present minor amounts of Si in their EDS data (Table 3); suggesting the latter are voids after the liberation of similar shaped (or the same) residents, and the Si interference is a result of left-over micro or nano- particles/fragments in these voids. On the other hand, the shapes of these negative crystals are also comparable to those of the C-bearing (CO_2 and CH_4) fluid inclusion examples previously reported from the chromitites (Ben Secours, New Caledonia; cf. Johan et al., 2017), and resemble to pits after the removal of fluid inclusions.

DISCUSSION

Summary of the previous evidence on UHP origin, deep mantle recycling of chromitites and the importance of the new in-situ findings from Orhaneli and Harmancık chromitites

There are several studies on the ophiolitic chromitites that report the ex-situ and in-situ clues for the possible UHP conditions. The first major evidence on UHP history of chromitites was the observation of UHP minerals as in-situ or separated grains. These observations included phases like diamond, moissanite and coesite from peridotites and podiform chromitites in different ages and orogenic belts (Yang et al., 2007; Liang et al., 2014; Howell et al., 2015; Robinson et al., 2015; Tian et al., 2015; Yang et al., 2015a; Lian et al., 2017). Arai (2010; 2013) and Arai and Miura (2016) suggested a deep mantle recycling process for the formation of these UHP phases in the ordinary low-pressure igneous chromitites, including downward and upward mantle convection processes that convert the C-bearing fluid inclusions in the mantle to micro-diamonds via UHP metamorphism. Moissanite (natural SiC) also forms at ultra highly reducing (UHR) conditions with the oxygen fugacity at least five to six log units below IW buffer (Mathez et al. 1995; Schmidt et al., 2014; Ulmer et al., 1998; Lian et al., 2017) and the presence of this phase in the podiform chromitites is interpreted as xenocrysts that possibly have a lower mantle origin and incorporated into the chromitites (cf. Trumbull et al., 2009).

Several other notable in-situ/ex-situ evidences from the UHP chromitites were also reported elsewhere. Lately, Griffin et al. (2016) have discussed and summarized the evidence of Transition Zone metamorphic conditions from the

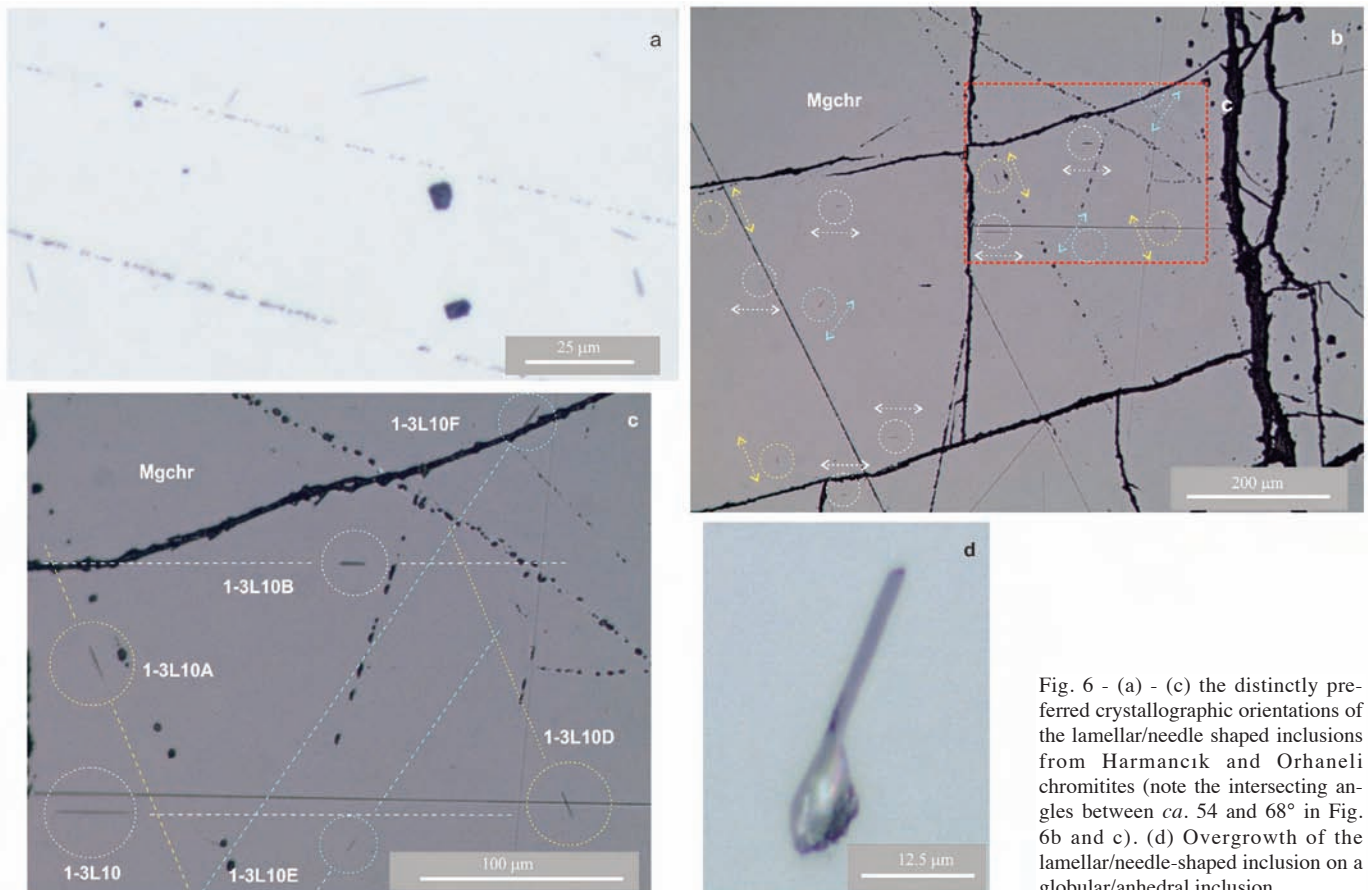


Fig. 6 - (a) - (c) the distinctly preferred crystallographic orientations of the lamellar/needle shaped inclusions from Harmancık and Orhaneli chromitites (note the intersecting angles between *ca.* 54 and 68° in Fig. 6b and c). (d) Overgrowth of the lamellar/needle-shaped inclusion on a globular/anhedra inclusion.

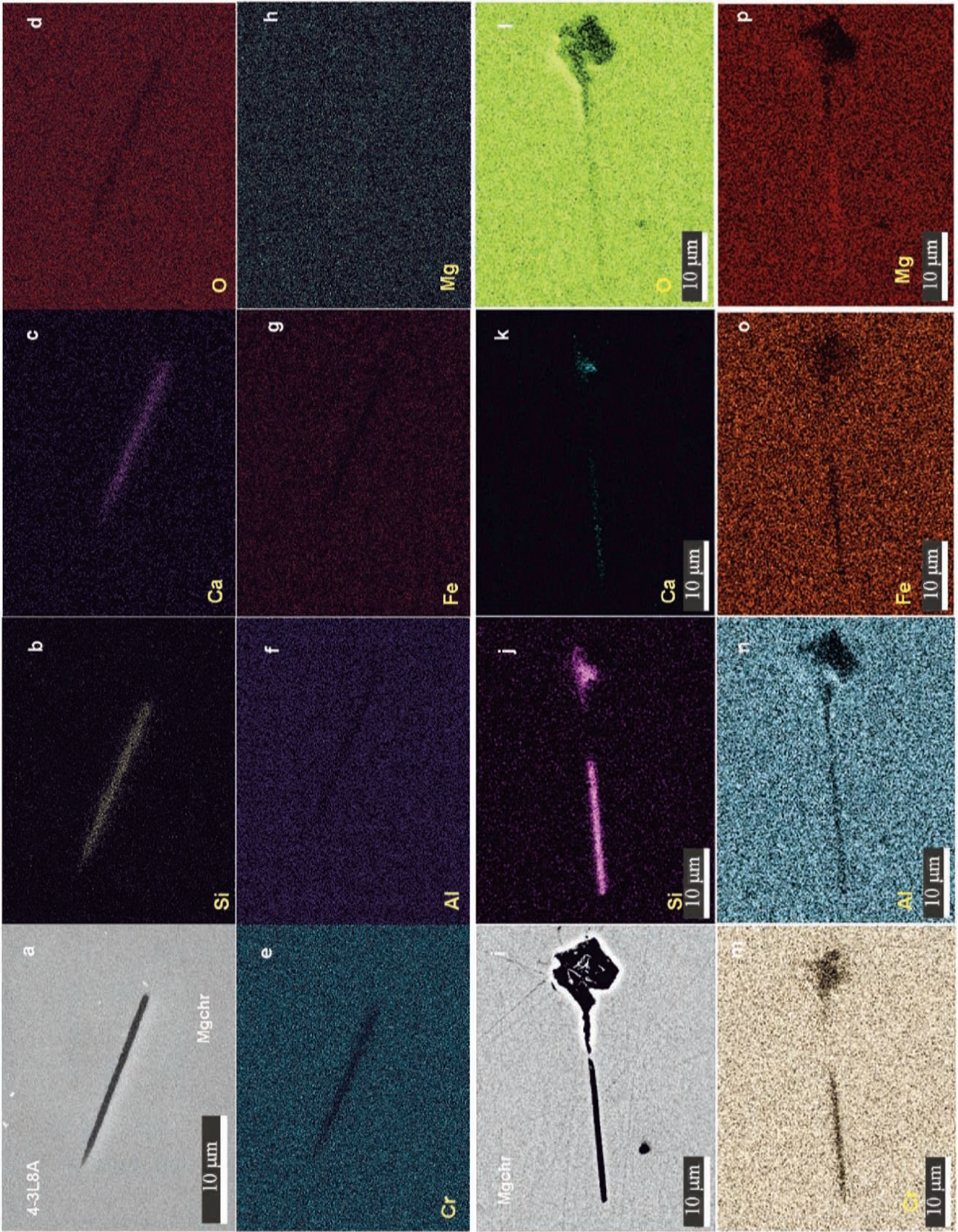


Fig. 7 - (a) to (p) BSE images and X-Ray elemental maps of lamellar/needle-shaped silicate micro-inclusion from Orhaneli and Harmancik chromitites. (a) and (i) show silicate micro-lamellae/needles from Orhaneli and Harmancik chromitites, respectively.

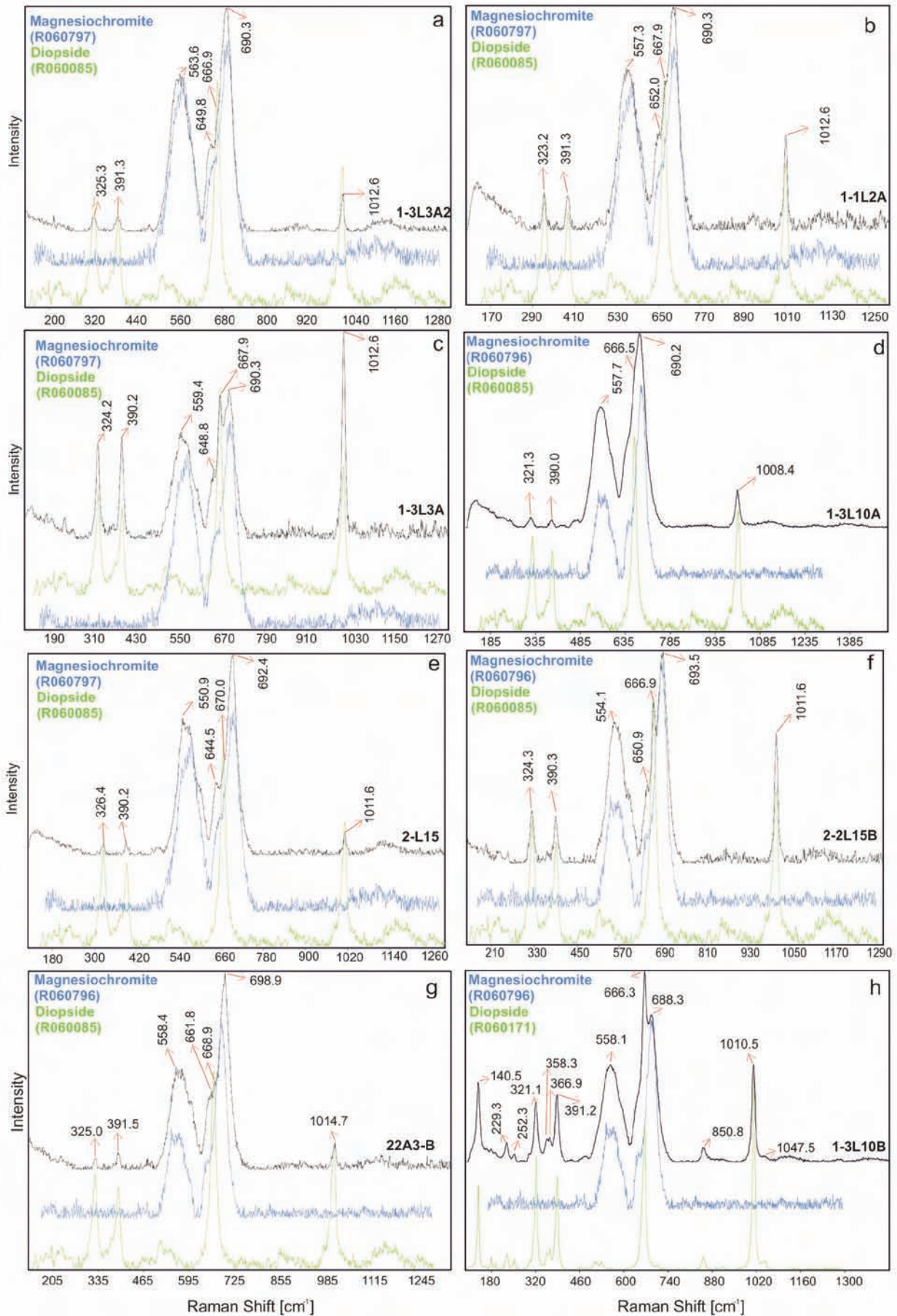


Fig. 8 - (a) to (h) Raman spectra of some of the relatively larger lamellar/needle-shaped micro inclusions within magnesiochromite hosts of the Orhaneli and Harmançik chromitites. The reference spectra used for comparison of the magnesiochromite and diopside peaks are shown in blue and green lines, respectively together with their RRUF ID-numbers (<http://rruff.info>).

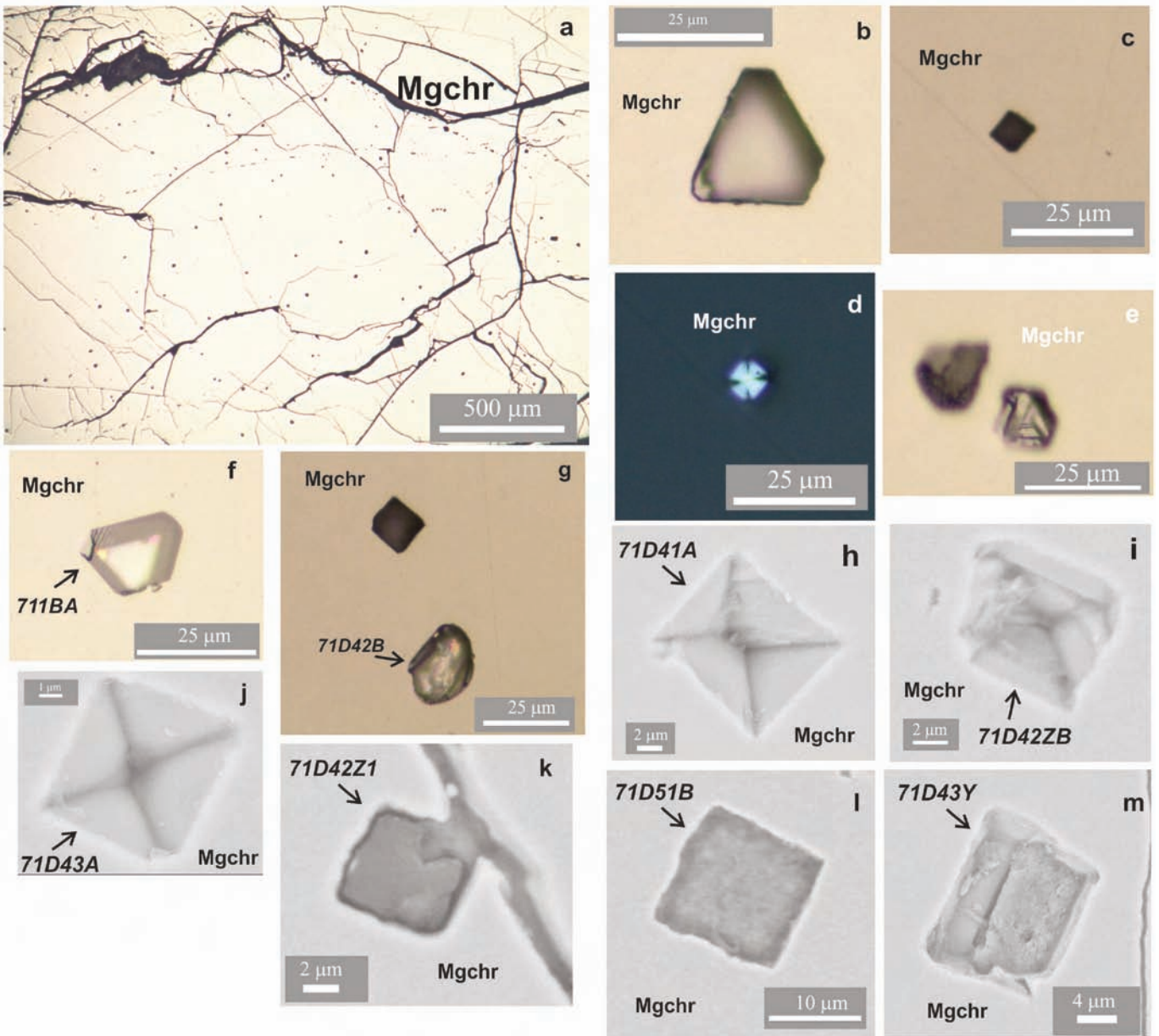


Fig. 9 - (a) “Peppered-like” appearance of the chromite nodule within the dunitic orbicules of the multi-textured Harmančík chromitite sample. (b) to (f) reflected light images of the cubic/octahedral, macle shaped and anhedral features encountered in the same sample. (d) and (e) are a slightly defocused images, the former under crossed polars. (h) - (j) BSE images of negative crystals (voids) of cubic/octahedral form. (k) Possible magnesite and serpentine infill in a former negative crystal void, note the fissure juxtaposed to the feature. (l) and (m) cubic Mg-silicate inclusions within the magnesiochromite.

peridotites and shallow-beginning chromitites of the Yarlung-Zangbo Suture Zone (YZSZ, southern Tibet, China). They reported that, in addition to the already known existence of diamonds in the chromitites from Luobusa that suggests depths > 150 km, the YZSZ harzburgites present other characteristics of a lithospheric mantle originally modified at a shallow SSZ environment and later modified at greater depths (*ca.* ~ 410-660 km) with the subduction and exhumation processes (Griffin et al., 2016). The characteristics summarized by Griffin et al. (2016) included: (1) reaction zone of acicular kyanite and SiO₂ (coesite and an unknown amorphous material) between the silicate matrix and spherical Fe-Ti alloy and nano-phases of TiO₂ II (Yang, et al., 2007; Dobrzhinetskaya et al., 2009), suggesting depths > 300 km; (2) high Fe³⁺ contents of spinels containing abundant spherules of native Fe (Dobrzhinetskaya et al., 2009;

Ruskov et al., 2010; McGowan et al., 2015), suggesting once existence of Ca-ferrite structured polymorph of chromite requiring deep-mantle conditions; (3) abundant needles of SiO₂ (at least some determined as coesite), diopside and rarely enstatite with preferred crystallographic orientations (Yamamoto et al., 2009), suggesting inversion to chromite from a high-P Ca-ferrite structured polymorph; (4) mineral separates of a new cubic Mg-silicate (provisionally termed “BWJ” and defined as an inverse spinel -all Si in octahedral coordination- with minor Si excess, and Mg and Al deficiency) and their antigorite pseudomorphs within the chromites, suggesting subduction-dehydration under ringwoodite-wadsleyite formation conditions; and (5) findings of coarse symplectitic intergrowths of orthopyroxene + spinel ± clinopyroxene (e.g., Hebert et al., 2003; Xiong, 2015), interpreted to represent breakdown products of high-P majoritic

garnet. Another in-situ UHP evidence for the Luobusa (Tibet) chromitites reported by Arai and Miura (2016) was the “PACO” (Pull-Apart Chromite filled by Olivine) texture; a special texture defined in nodular chromitites which is characterized by pull-part cracks filled with fresh olivine crystals, optically continuous to the matrix olivines.

Unusual minerals such as diamonds, moissanite and “silicates of octahedral pseudomorph”, and various crustal phases (rutile, monazite, zircon etc.) have been lately reported from the mineral separates of the Pozanti-Karsanti ophiolitic chromitites (as ex-situ phases) of southern Turkey (Lian et al., 2017) and these were affiliated with deep-mantle origin and ultra-reducing conditions. However, there were no other reports of ex-situ or in-situ UHP evidences from any other Turkish chromitites. As it is hard to find these UHP phases in-situ, certain special mineral separation techniques (such as selfFrag -electrostatic rock disaggregation facility-, hydroseparation, etc.) must be used to obtain fractions including these mineral species. Unfortunately, these special sample preparation facilities are not ubiquitously available. The study on the Orhaneli and Harmancık chromitites (northwestern Turkey) however, shows the first direct in-situ evidence for the UHP history of northwestern Turkish chromitites by using simple polished blocks prepared from the ophiolitic chromitites. The main evidence determined in this study for the UHP history is the existence of lamellae/needle-shaped diopside micro-inclusions in these chromitites.

The presence of lamellar/needle-shaped clinopyroxene and SiO_2 inclusions with preferred crystallographic orientations located in chromite have recently been recognized as one of the in-situ indicators of UHP conditions that once affected the host chromite (cf. Yamamoto et al., 2009; Satsukawa et al., 2015; Griffin et al., 2016). Previous TEM or EBSD studies performed in such inclusions well-established the topotaxial relationships with their host chromite, suggesting that they are exsolved from their host (cf. Yamamoto et al., 2009; Satsukawa et al., 2015; Griffin et al., 2016). The occurrence of these inclusions is mainly explained with the inversion of a higher-pressure Ca-ferrite structure (CF-type chromite) to the lower pressure cubic chromite structure resulting in exsolution products of clinopyroxene (mainly diopside) and SiO_2 (as coesite) within the final host due to the insoluble character of Ca and Si in the cubic chromite (Griffin et al., 2016). Yamamoto et al. (2009) reported that they encountered these lamellae/needle-shaped inclusions in the massive-, nodular-, and dunitic-orbicular-chromitites from Luobusa, and noted that the disseminated and banded types lack these lamellae/needles suggesting a multi-stage development from ultrahigh-pressure to low-pressure magmatic processes. Arai (2013) discussed the possibilities of either a direct ultrahigh-pressure magmatic formation or recycling origin for the UHP chromitites and noted that it is much easier to recycle the low-P chromitite-dunite-harzburgite set through mantle, than converting a primarily high-P chromitite-ringwoodite rock set to the chromitite-dunite envelope-harzburgite host basic structure by decompression. During compression, the primary low-P hydrous mineral inclusions in chromite would possibly be broken down leaving residual diopside component that may further be dissolved in the high-P Ca-ferrite structured chromite, and reappear as pyroxene exsolution lamellae in chromite during decompression towards the shallower levels (cf. Yamamoto et al., 2009; Arai, 2013). The chromitite would revert to its original mineralogy of olivine and cubic chromite and sometimes preserves the initial nodular/orbic-

ular magmatic texture with only significant modification (tightening) in the chromite packing of the nodules (Arai, 2013 and the references therein). This way the initial igneous textures would have been basically preserved even during deep recycling though the Transition Zone because of possible absence of reactions between olivine and chromite and their high-P polymorphs (Arai, 2013).

Several oriented lamellar/needle-shaped diopside micro-inclusions are observed in Orhaneli and Harmancık chromitites. The oriented inclusions have a tendency to have either a topotactic relationship with the matrix phase or an orientation minimizing the dimensional misfit between the strain-free lattices at the phase boundary (Fleet and Arima, 1985 and references therein). Topotaxial or epitaxial relationships may be constructed by extensive mineralogical studies and/or by application of advanced mineralogical methods such as Transmission Electron Microscopy (TEM) or Electron Backscatter Diffraction (EBSD). However, no direct evidence is obtained from Orhaneli and Harmancık chromitites yet to present here for a clear topotaxial relationship between these diopside micro-inclusions and their host chromites. Still, their preferred crystallographic orientation patterns within the host chromites are quite characteristic. Moreover, over-growth of a lamellar/needle-shaped diopside inclusion on a globular/anhydral diopside (Fig. 6d) in a chromite from the Harmancık chromitites is similar to the textural relationship described from the chromitite samples from Luobusa (cf. Yamamoto et al., 2009). Yamamoto et al. (2009) suggest that this kind of over-growth relationship indicates the late stage character of the lamellar/needle-shaped inclusions and marks the continuous decompression in the upwelling-mantle. Hence, given the resemblance of the lamellar/needle-shaped diopside inclusions from the current study with the previous examples from other UHP chromitites from the eastern segment of Tethyan domain, they are interpreted as the first and main microscopic in-situ evidence of UHP -and possibly a deep mantle recycling- history for the Orhaneli and Harmancık chromitites (northwestern Turkey). As the chromitite samples implying the UHP history are taken randomly from the field and studied polished sections are prepared from the slightly thicker parts of the chromitite bands and schlierens, no further significant macroscopic field evidence for UHP nature has been noted.

Still, describing the presence of diopside micro-lamellae/needles in the Orhaneli chromitites brings forward another topic of debate. Similar diopside micro-lamellae/needles have been already described in several examples from the upper mantle chromitites within the mantle tectonites (as well as in the Harmancık chromitites of the current study), but none has been reported from the Moho Transition Zone (MTZ) chromitites yet. Thus, the presence of these diopside micro-lamellae within the banded chromitites of the Orhaneli Ophiolite Complex (a remnant paleo-MTZ) should be further discussed. A periodic magma replenishment process was suggested for the repetitive cycling of the mafic-ultramafic cumulate units defined in the Orhaneli Ophiolite Complex (e.g., Sarıfakıoğlu et al., 2009). A similar replenishment process was also described by Zhang et al. (2017) for the occurrence of the chromitites in the paleo-MTZ from Kop Ophiolite (NE Turkey). Zhang et al. (2017) concluded that the oversaturation of chromite in the Kop MTZ could not be reached by magmatic differentiation alone, and was most likely due to mixing of more evolved magmas with more primitive magmas inducing formation of interlayered chromitites and dunites. Hence, one may take

into account the migration of deep mantle recycled material along with the upwelling and ponding melts in the MTZ, similarly to the processes suggested for the upper mantle chromitites by Arai (2013).

It may be speculated that recycled fragments of UHP chromitites (converted from low-pressure to UHP with possible pathways suggested by Arai, 2013) migrating from the deeper mantle may be entrapped in the upwelling primordial melts feeding the evolved magmas ponding in the MTZ. The subsequent oversaturation and accumulation of chromite (that will form the chromitite bands within the cumulate dunite) would enclose and incorporate these relics. Such a scenario may seem to be supported by the complex origin of the Orhaneli chromitites (compositionally akin to the podiform chromitites with boninitic to island arc tholeiitic character while showing a cumulate structure; cf., Uysal et al., 2015), and by the mixed mantle and cumulate characteristics defined for the Orhaneli ultramafic suite (cf. Uysal et al., 2017). However, further studies must be carried out in order to clarify the possible processes and mechanisms behind this issue.

**Dunitic orbicular texture:
in search of a possible macroscopic textural
field evidence for UHP chromitites?**

As the UHP phases are rare and hard to obtain from the chromitites, discriminating between the UHP and non-UHP chromitites in the field and/or under the microscope using other evidence is essential (cf. Arai and Miura, 2016). Arai and Miura (2016) suggested the formation of the “PACO” texture in chromitites as an additional evidence for UHP origin. On the other hand, Yamamoto et al., (2009; 2015) reported that the silicate exsolution lamellae (e.g., coesite, clinopyroxene and $MgSiO_3$ phase) are restricted in nodular and massive-type chromitites and are not found in the disseminated chromitites from Luobusa. Yamamoto et al. (2009; 2015) also noted that the dunitic orbicular type chromitite comprised both the high-pressure (nodular chromite nuclei including silicate exsolution lamellae and surrounded by an outer shell of olivine) and low-pressure type (e.g., disseminated chromitites with no silicate exsolution lamellae and scattered in the interstitial part of the matrix) chromitites, suggesting a multi-stage development from ultra-high pressure to low-pressure magmatic processes. Yamamoto et al. (2009; 2015) further indicated that nodular type chromites with abundant silicate-exsolutions are gradually modified into disseminated-type chromites in their morphology and exsolution abundance. Such findings and considerations brings up the question of whether there is a link between deep mantle recycling and dunitic orbicular texture forming processes.

Orbicular chromitite is a rather rare texture, specific to the ophiolitic chromitites. This texture is mainly described to comprise dunitic orbicules with chromite aggregate nuclei in a matrix of mixed olivine and chromite grains (Bowles et al., 2011). However, there are many occasional examples resembling the nodular chromitites. These examples typically comprise dunitic orbicules lacking significant chromite aggregate nuclei, surrounded by rather thin chromite shells that are embedded in a dunitic matrix. Thus, to distinguish between these two different orbicular types, the former type has been addressed as dunitic orbicular type in this study (as also done by Yamamoto et al., 2009; 2015). Ophiolitic chromitites within mantle peridotite massifs scattered along northern and

southern Turkish ophiolitic belts rarely show the orbicular texture along with much common disseminated, semi-massive, massive and nodular textures. However, occurrence of dunitic orbicular texture is much rarer.

Several examples of such dunitic orbicular texture were previously reported elsewhere around the world (e.g., Johnston, 1936; Rynearson and Smith, 1940; Bastin, 1950). Simply pronounced as orbicular ore by Johnston (1936) and Rynearson and Smith (1940), the texture is described as orbicules (or spheroidal units) made of masses of chromite nuclei surrounded by elongated olivine shells (sometimes alternating shells of chromite and olivine), further surrounded either by minor to abundant interstitial masses of chromite. Johnston (1936) concluded that the chromite nuclei are older than the enclosing dunitic orbicule and belong to an earlier magmatic stage, whilst the interstitial chromite enclosing the orbicules is younger and may belong to a late magmatic stage, with no specific descriptions on the nature of the stages. Rynearson and Smith (1940) also related the orbicular chromite to have resulted from replacement of the original structure in the peridotites, giving no further details. It should be noted that no microscopic studies are conducted in these work, thus there are no microscopic/petrographic data on these chromitites studied. Still, multi-stage nature of the texture is also recognized by these authors.

Several different processes such as mechanical coalescence of olivines and chromites to rounded nodules in turbulent magma conduits, the presence of immiscible oxide melts under mantle conditions, or hydrothermal activity are indicated by different authors for the origin of nodular and orbicular chromitites (cf. Ballhaus, 1998 and references therein). Ballhaus (1998) experimentally duplicated nodular chromite textures on a microscale and suggested that the nodular and orbicular ore textures form where low-silica, low-viscosity, high-pressure melts (from different mantle depths) pool and mingle within more siliceous and more viscous low-pressure liquid reservoir (e.g., conduits and/or interconnected 3-dimensional networks of channels in the shallow lithosphere).

Being inspired by the above given literature on UHP chromitites and the nodular/orbicular textures, one can argue for a connection between deep mantle recycling and dunitic orbicular textures. The best research medium for this argument in this study is the multi-textured Harmancık chromitite sample presenting dunitic orbicular, semi-massive and massive textures. In light of these previous studies, the step-by step textural interpretation of this sample suggests that there are at least two stages of chromite formations: (1) the first stage tightly packed nodular chromite nuclei within the dunitic orbicules, (2) the later stage chromite of the semi-massive to massive (again finally tightly packed) chromitite. The first stage chromitite can clearly be traced to be finally incorporated within the later stage chromitite. No in-situ silicate micro-exsolution lamellae/needles or any other unusual high pressure minerals are detected in this sample, either none exist or they are overlooked. However, the presence of euhedral/subhedral cubic/octahedral silicate inclusions and negative crystal shapes may be argued for another additional in-situ evidence for the UHP (and probably deep mantle recycling) history of the Harmancık chromitites.

The morphological descriptions from the negative crystals of cubic form and limited compositional data from these silicate inclusions in this Harmancık sample closely resemble to the previously defined cubic Mg-silicates (or their antigorite counterparts within the chromites) from two other

important Tethyan ophiolitic chromitite locations (Luobusa and Pozantı-Karsantı; cf. Griffin et al., 2016; Lian et al., 2017). These hydrous and anhydrous phases were not identified in-situ (e.g., Griffin et al., 2016; Lian et al., 2017), but were correlated with faceted antigorite aggregates embedded (sometimes along rough linear arrays) within the chromitites including abundant exsolution needles (Griffin et al., 2016). The ones in the Luobusa chromitites were interpreted to be formed after a high-pressure cubic olivine pseudomorph, possibly ringwoodite (e.g., Robinson et al., 2004; Griffin et al., 2016; Lian et al., 2017). They were mainly interpreted to be derived from antigorites entrapped within chromitite during shallow mantle residence (under low-P conditions), later necked down and annealed into inclusions of negative crystals being dehydrated during subduction and/or its residence in Transition Zone (under high-P conditions) (cf. Griffin et al., 2016). Similar cubic/octahedral Mg-silicate findings were also recently reported by Lian et al. (2017) from the Pozantı-Karsantı ophiolitic chromitites (southern Turkey) along several diamond, moissanite and crustal minerals, also suggesting deep mantle origin for these ophiolitic chromitites. Thus, the occurrence of these cubic Mg-silicates and, if considered as leftover voids after the same residents, the negative crystals of cubic/octahedral form found in this Harmancık sample may be speculated as other indicators of the UHP and deep mantle recycling history from the Harmancık chromitites. Minor amounts of Si in the EDS data obtained from these negative crystals also support this interpretation.

However, the coexistence of K-Na-Ca and Mg bearing silicates (possibly pargasite?) in the same chromite grains stand as a problem for this consideration, since such phases ubiquitously found in low-P chromitites are regarded as the main suppliers of incompatible elements for the formation of silicate lamellae in UHP chromitites during decompression; the UHP chromitites are expected to be free of such inclusions (cf. Arai, 2013; Arai and Miura, 2016). Moreover, the negative crystals of cubic/octahedral form also resemble to the shapes of the C-bearing (CO₂ and CH₄) fluid inclusion examples embedded in chromites from New Caledonia (Johan et al., 2017). Although no fluidal species (liquid or gas) currently reside in any of these inclusions, they may also be speculated to be negative crystals leftover after the removal of fluid inclusions, possibly during the sample preparation processes. Hence, due to these conflicting possibilities discussed above, no further speculations can be made on the nature of these findings until further evidence is obtained. Future research should include the further textural, chemical, crystallographic studies on these chromitites for finding a field evidence for UHP nature, as well as the search for unusual UHP phases (such as diamond, moissanite etc.).

CONCLUSIONS

The studied micro-inclusions hosted in magnesian chromites of Orhaneli and Harmancık chromitites in northwestern Turkey include several randomly distributed globular forsterite and diopside, selectively oriented lamellar/needle-shaped diopside and other euhedral/subhedral silicate inclusions (including cubic Mg-bearing silicates, and Na-K-Ca and Mg bearing silicates), cubic/octahedral structured negative crystals, and IPGE bearing PGM and BMS. Although no other unusual ultrahigh-pressure (UHP) phases

(e.g., diamonds, moissanite, coesite etc.) are currently encountered, the occurrence of the selectively oriented lamellae/needles of diopside detected are interpreted as first in-situ evidence of UHP and deep mantle recycling history for the Orhaneli and Harmancık chromitites. The presence of the diopside micro-lamellae/needles in Orhaneli chromitites located within the cumulate dunites may be speculated to be affiliated with entrapment of recycled relicts/fragments of UHP chromitites in the upwelling primordial melts feeding the evolved magmas ponding in the MTZ. Future studies should focus on acquiring data on the most possible processes and mechanisms behind this question and explore the possibility of the occurrence of diamond, moissanite and other unusual UHP phases in these regions. Occurrences of cubic/octahedral Mg-silicates and the negative crystals of cubic form determined in a multi-textured (presenting dunitic orbicular, semi-massive and massive textures) Harmancık sample is also questioned for a possible link between the textural evolution of chromitites and the UHP processes, and possibilities for finding a macroscopic evidence for discrimination of UHP chromitites in the field. However, due to some conflicting findings, it is concluded that more data are also needed for reaching a final solution.

ACKNOWLEDGEMENTS

The author is grateful to the Exploration Manager and Geologist İbrahim BOZKURT for his kind helps and assistance during chromitite sampling from CVK Group's (CVK Mineral ve Madencilik A.Ş.) Harmancık (Bursa, Turkey) operation. Akın Fidan, Emre Kavvasoğlu, Olcay Doğan, Sami Ekiz and Mert Can Şahin are thanked for their valuable assistance during the field studies and sampling around Orhaneli and Harmancık (Bursa, Turkey) regions. The author also thanks Dr. Jing-Sui Yang, an anonymous reviewer and Dr. Alessandra Montanini for their constructive criticism and reviews. This research did not receive any specific grant from funding agencies in the public, commercial, or not-for-profit sectors.

REFERENCES

- Ahmed A.H. and Arai S., 2002. Unexpectedly high-PGE chromitite from the deeper mantle section of the northern Oman ophiolite and its tectonic implications. *Contrib. Miner. Petr.*, 143: 263-278.
- Akbulut M., González-Jiménez J.-M., Griffin W.L., Belousova E., O'Reilly S.Y., McGowan N. and Pearson N.J., 2016. Tracing ancient events in the lithospheric mantle: A case study from ophiolitic chromitites of SW Turkey. *J. Asian Earth Sci.*, 119: 1-19.
- Akbaş B., Akdeniz N., Aksay A., Altun İ., Balcı V., Bilginer E., Bilgiç T., Duru M., Ercan T., Gedik İ., Günay Y., Güven İ.H., Hakyemez H. Y., Konak N., Papak İ., Pehlivan Ş., Sevin M., Şenel M., Tarhan N., Türkecan A., Ulu Ü., Uğuz M.F., Yurtsever A. and others, 2001. Geological Map of Turkey. General Directorate of Mineral Research and Exploration [Maden Tetkik ve Arama Genel Müdürlüğü - MTA] Publ. Ankara, Turkey.
- Arai S., 2010. Possible recycled origin for ultrahigh-pressure chromitites in ophiolites. *J. Miner. Petr. Sci.*, 105: 280-285.
- Arai S., 2013. Conversion of low-pressure chromitites to ultrahigh-pressure chromitites by deep recycling: a good inference. *Earth Planet. Sci. Lett.*, 379: 81-87.
- Arai S. and Matsukage K., 1996. Petrology of the gabbro-troctolite-peridotite complex from Hess Deep, equatorial Pacific: implications for mantle-melt interaction within the oceanic lithosphere. *ODP Sci. Res.*, 147: 135-155.

- Arai S. and Matsukage K., 1998. Petrology of a chromitite micro-pod from Hess Deep, equatorial Pacific: a comparison between the abyssal and alpine-type podiform chromitites. *Lithos*, 43: 1-14.
- Arai S. and Miura M., 2015. Podiform chromitites do form beneath mid-ocean ridges. *Lithos*, 232: 143-149.
- Arai S. and Miura M., 2016. Formation and modification of chromitites in the mantle. *Lithos*, 364: 277-295.
- Arai S. and Yurimoto H., 1994. Podiform chromitites of the Tari-Misaka ultramafic complex, southwestern Japan, as mantle-melt interaction products. *Econ. Geol.*, 89: 1279-1288.
- Arai S. and Yurimoto H., 1995. Possible sub-arc origin of podiform chromitites. *Isl. Arc*, 4: 104-111.
- Arai S., Kadoshima K. and Morishita T., 2006. Widespread arc-related melting in the mantle section of the northern Oman ophiolite as inferred from detrital chromian spinels. *J. Geol. Soc. London*, 163: 869-879.
- Ballhaus C., 1998. Origin of podiform chromite deposits by magma mingling. *Earth Planet. Sci. Lett.*, 156: 185-193.
- Bastin E.S., 1950. Interpretation of Ore Textures. *Geol. Soc. Am. Mem.*, 45, 101 pp.
- Berger E.T. and Vannier M., 1984. Dunite inclusions in the alkali basalts of oceanic islands: Petrological approach. *Bull. Minér.*, 107 (5): 649-663.
- Borchert H. and Uzkuş İ., 1967. Harmancık (Bursa ili) kuzeybatısındaki krom cevheri yatakları [Chrome ore deposits to the northwest of Harmancık (Bursa)]. *Maden Tetkik ve Arama Dergisi*, 68: 49-63. (in Turkish with English abstract).
- Boudier F. and Nicolas A., 1972. Fusion partielle gabbroïque dans la lherzolite de Lanzo (Alpes piémontaises) [Gabbroic partial melting in the Lanzo lherzolite (Piedmont Alps)]. *Bull. Suisse Minér. Pét.*, 52: 39-56.
- Boudier F., Nicolas A. and Bouchez J.L., 1982. Kinematics of oceanic thrusting and subduction from basal sections of ophiolites. *Nature*, 296: 825-828.
- Bowles J.F.W., Howie R.A., Vaughan D.J. and Zussman J., 2011. Rock-forming minerals. Non-silicates: oxides, hydroxides and sulfides. *Geol. Soc. London*, Vol. 5A, 2nd Ed., 920 pp.
- Brown M., 1980. Textural and geochemical evidence for the origin of some chromite deposits in the Oman ophiolite. In: A. Panayiotou (Ed.), *Ophiolites: Proceed. Intern. Ophiolite Symp.*, Cyprus, 1979. *Geol. Survey Dept.*, Cyprus, p.714-721.
- Cassard D., Nicolas A., Rabinowicz M., Moutte M., Leblanc M. and Prinzhofer A., 1981. Structural classification of chromite pods in southern New Caledonia. *Econ. Geol.*, 76: 805-831.
- Catlos E.J. and Çemen I., 2005. Monazite ages and evolution of the Menderes Massif, western Turkey. *Intern. J. Earth Sci. (Geol. Rund.)*, 94: 204-217, doi: 10.1007/s00531-005-0470-7.
- Ceuleneer G. and Nicolas A., 1985. Structures in podiform chromite from Maşad district (Sumail ophiolite, Oman). *Miner. Dep.*, 20: 177-185.
- Dickey J.S., 1975. A hypothesis of origin for podiform chromite deposits. *Geochim. Cosmochim. Acta*, 39: 1061-1074.
- Dilek Y. and Furnes H., 2009. Structure and geochemistry of Tethyan ophiolites and their petrogenesis in subduction roll-back systems. *Lithos*, 113: 1-20.
- Dobrzhinetskaya L.F., Wirth R., Yang J.S., Ian D., Hutcheon P.K. and Green H.W., 2009. High-pressure highly reduced nitrides and oxides from chromitite of a Tibetan ophiolite. *Proceed. Nat. Acad. Sci. USA*, 106: 19233-19238.
- Dziewonski A.M. and Anderson D.L., 1981. Preliminary reference Earth model. *Phys. Earth Planet. Inter.*, 25: 297-356.
- Elthon D., Casey J.F. and Komor S., 1982. Mineral chemistry of ultramafic cumulates from the North Arm Mountain Massif of the Bay of Islands Ophiolite: Implication for high pressure fractionation of oceanic basalts. *J. Geophys. Res.*, 87: 8717-8734.
- Fidan A., 2016. Bursa İli Çevresinde Yer Alan Kromit Yataklarının Mineralojisi ve Cevher Mikroskopisinin İncelenmesi. B. Sci. Thesis, Dokuz Eylül University, İzmir, Turkey, 85 p. (in Turkish with English abstract).
- Fleet M.E. and Arima M., 1985. Oriented hematite inclusions in sillimanite. *Am. Miner.*, 70: 1232-1237.
- González-Jiménez J.-M., Griffin W.L., Proenza J.A., Gervilla F., O'Reilly S.Y., Akbulut M., Pearson N.J. and Arai S., 2014. Chromitites in ophiolites: how, where, when, why?, Part II. A review and new ideas on the crystallization of chromitites. *Lithos*, 189: 140-158.
- Greenbaum D., 1977. Textural, structural and chemical evidence of the origin of chromite in the Troodos ophiolite complex, Cyprus. *Econ. Geol.*, 72: 1175-1194.
- Griffin W.L., Afonso J.C., Belousova E.A., Gain S.E., Gong X.-H., González-Jiménez J.M., Howell D., Huang J.-X., McGowan N., Pearson N.J., Satsukawa T., Shi R., Williams P., Xiong Q., Yang J.-S., Zhang M. and O'Reilly S.Y., 2016. Mantle recycling: transition zone metamorphism of Tibetan ophiolitic peridotites and its tectonic implications. *J. Petr.*, 1-30, doi: 10.1093/petrology/egw011.
- Güllaşlı Ö.F., 1996. Mineralogy, petrology and origin of ultramafics in Orhaneli (Bursa) Ophiolite Complex. M. Sci. Thesis, Graduate School of Natural and Applied Sci., Dokuz Eylül Univ., Turkey, 118 pp.
- Harris N.B.W., Keller S.P. and Okay A.İ., 1994. Post-collision magmatism and tectonics in northwest Turkey. *Contrib. Miner. Petr.*, 17: 241-252.
- Hebert R., Huot F., Wang C. and Liu Z., 2003. Yarlung Zangbo ophiolites (Southern Tibet) revisited: Geodynamic implications from the mineral record. In: Y. Dilek and P. Robinson (Eds.), *Ophiolites in Earth history*. *Geol. Soc. London Spec. Publ.*, 218: 165-190.
- Howell D., Griffin W.L., Yang J., Gain S., Stern R.A., Huang J., Jacob D.E., Xu X., Stokes A.J. and O'Reilly S.Y., 2015. Diamonds in ophiolites: Contamination or a new diamond growth environment? *Earth Planet. Sci. Lett.*, 430: 284-295.
- Huang E., Chen C.H., Huang T., Lin E.H. and Xu J., 2000. Raman spectroscopic characteristics of Mg-Fe-Ca pyroxenes. *Am. Miner.*, 85: 473-479.
- Huang Z., Yang J.S., Robinson P.T., Zhu Y.W., Xiong F.H., Liu Z., Zhang Z.M. and Xu W., 2015. The discovery of diamond in chromitites of the Hegenshan ophiolite, Inner Mongolia, China. *Acta Geol. Sinica*, 89: 341-350.
- Irvine T.N., 1975. Crystallization sequences in the Muskox intrusion and other layered intrusions. 2. Origin of chromitite layers and similar deposits of other magmatic ores. *Geochim. Cosmochim. Acta*, 39: 911-1020.
- Irvine T.N., 1977. Origin of chromitite layers in the Muskox intrusion and other stratiform intrusions: A new interpretation. *Geology*, 5: 273-277.
- Irvine T.N., 1978. Chromite crystallization in the joint Mg₂SiO₄ - CaMgSi₂O₆ - CaAl₂Si₂O₈ - MgCr₂O₄ - SiO₂. *Carnegie Inst. Geophys. Lab. Rep.*, 1976-1978: 465-472.
- Jackson E.D., Green H.W. and Moores E.M., 1975. The Vourinos ophiolite, Greece: Cyclic units of lineated cumulates overlying harzburgite tectonite. *Geol. Soc. Am. Bull.*, 86: 390-398.
- Johan Z., 1986. Chromite deposits in the Massif du Sud ophiolite, New Caledonia: genetic considerations. In: W. Petrascheck, S. Karamata, G.G. Kravchenko, Z. Johan, M. Economou and T. Engin (Eds.), *Chromites UNESCO's IGCP-197 project "Metallogeny of Ophiolites"*, Theophrastus Publications, Athens, p. 311-339.
- Johan Z. and Le Bel L., 1980. Origin of layers and pods of chromite in ophiolite complexes. 26th Intern. Geol. Cong. Paris, Abstr., 3: 950.
- Johan Z., Dunlop H., Le Bel L., Robert J.L. and Volfinger M., 1983. Origin of chromite deposits in ophiolite complexes: Evidence for a volatile and sodium-rich reducing fluid phase. *Fortschr. Miner.*, 61: 105-107.
- Johan Z., Martin R.F. and Ettler V., 2017. Fluids are bound to be involved in the formation of ophiolitic chromite deposits. *Eur. J. Miner.*, PrePubl., doi: 10.1127/ejm/2017/0029-2648
- Johnston W.D. Jr., 1936. Nodular, orbicular, and banded chromite in northern California. *Econ. Geol.*, 31: 417-427.

- Juteau T., 1975. Les ophiolites des Nappes d'Antalya (Taurides occidentales, Turquie). Petrologie d'un fragment de ancienne croute oceanique tethysienne. *Sci. Terre Nancy Mem.*, 32, 692 pp.
- Kelemen P.B., 1989. Reaction between ultramafic rock and fractionating basaltic magma, 1. Phase relations, the origin of calc-alkaline magma series and the formation of discordant dunite. *J. Petr.*, 31: 51-98.
- Laetsch T. and Downs R., 2006. Software for identification and refinement of cell parameters from powder diffraction data of minerals using the RRUFF project and American Mineralogist Crystal Structure Databases. 19th General Meet. Intern. Miner. Ass., Kobe, Japan, July 2006. Abstr.: 23-28
- Lago N.L., Rabiowicz M. and Nicolas A., 1982. Podiform chromite orebodies: A genetic model. *J. Petr.*, 23: 103-125.
- Leblanc M. and Ceuleneer G., 1992. Evidence for chromite crystallization in a multicellular magma flow: Evidence from a chromitite dike in the Oman ophiolite. *Lithos*, 27 (4): 231-258.
- Leblanc M. and Nicolas A., 1992. Ophiolitic chromitites. *Intern. Geol. Rev.*, 34 (7): 653-686.
- Lian D., Yang J.Y., Dilek Y., Wu W., Zhang Z., Xiong F., Liu F. and Zhou W., 2017. Deep mantle origin and ultra-reducing conditions in podiform chromitite: Diamond, moissanite and other unusual minerals in podiform chromitites from the Pozanti-Karsanti ophiolite, southern Turkey. *Am. Miner.*, 102: 1101-1113.
- Liang F., Xu Z. and Zhao J., 2014. In-situ moissanite in dunite: deep mantle origin of mantle peridotite in Luobusa Ophiolite, Tibet. *Acta Geol. Sinica (English Ed.)*, 88(2): 517-529.
- Mathez E.A., Fogel R.A., Hutcheon I.D. and Marshintsev V.K., 1995. Carbon isotopic composition and origin of SiC from kimberlites of Yakutia, Russia. *Geochim. Cosmochim. Acta*, 59 (4): 781-791.
- Maurel C. and Maurel P., 1982. Experimental study of the solubility of chromium in mafic silicate baths and its partitioning between liquid and coexisting minerals: Conditions of existence of chromian spinel. *Bull. Minér.*, 105: 640-647.
- McGowan N.M., Griffin W.L., González-Jiménez J.M., Belousova E.A., Afonso J., Shi R., McCammon C.A., Pearson N.J. and O'Reilly S.Y., 2015. Tibetan chromitites: Excavating the slab graveyard. *Geology*, 43: 179-182.
- Miura M., Arai S., Ahmed A.H., Mizukami M., Okuno M. and Yamamoto S., 2012. Podiform chromitite classification revisited: a comparison of discordant and concordant chromitite pods from Wadi Hilti, northern Oman ophiolite. *J. Asian Earth Sci.*, 59: 52-61.
- MTA (General Directorate of Mineral Research and Exploration), 2002. 1:500.000 scaled Geological Map of Turkey, Ankara-Turkey.
- Nicolas A., 1986. A melt extraction model based on structural studies in mantle peridotites. *J. Petr.*, 27: 999-1022.
- Nicolas A., 1989. Structures of ophiolites and dynamics of oceanic lithosphere. Kluwer Academic Publ., Dordrecht, 367 p.
- Nicolas A. and Prinzhofer A., 1983. Cumulative or residual origin for the transition zone in ophiolites: Structural evidence. *J. Petr.*, 24: 188-206.
- O'Reilly S.Y. and Griffin W.L., 2013. Moho vs crust-mantle boundary: Evolution of an idea. *Tectonophysics*, 609: 535-546.
- Özen H., Çolakoglu A., Sayak H., Gültaşlı Ö.F., Başta Ö., and Sarıfakioğlu E., 2004. Ophiolitlere bağlı cevherleşmelerin araştırılması [The investigation of ophiolite-related mineralizations]. *Miner. Res. Explor. Inst. Turkey (MTA)*, Project no. 16B15. (in Turkish with English abstract).
- Robinson P.T., Bai W., Malpas J., Yang J., Zhou M., Fang Q., Hu X., Cameron S. and Staudigel H., 2004. Ultra-high pressure minerals in the Luobusa Ophiolite, Tibet, and their tectonic implications. *Geol. Soc. London Spec. Publ.*, 226: 247-272.
- Robinson P.T., Trumbull R.B., Schmitt A., Yang J., Li J., Zhou M., Erzinger J., Dare S. and Xiong F., 2015. The origin and significance of crustal minerals in ophiolitic chromitites and peridotites. *Gondw. Res.*, 27 (2): 486-506.
- Roeder P.L. and Reynolds I., 1991. Crystallization of chromite and chromium solubility in basaltic melts. *J. Petrol.*, 32: 909-934.
- Rollinson H. and Adetunji J., 2013. Mantle podiform chromitites do not form beneath midocean ridges: a case study from the Moho transition zone of the Oman ophiolite. *Lithos*, 177: 314-327.
- Rollinson H. and Adetunji J., 2015. The geochemistry and oxidation state of podiform chromitites from the mantle section of the Oman ophiolite: A review. *Gondw. Res.*, 27 (2): 543-554. doi: 10.1016/j.gr.2013.07.013.
- Ruskov T., Spirov I., Georgieva M., Yamamoto S., Green H.W., McCammon C.A. and Dobrzhinetskaya L.F., 2010. Mössbauer spectroscopy studies of the valence state of iron in chromite from the Luobusa massif of Tibet: implications for a highly reduced deep mantle. *J. Metam. Geol.*, 28: 551-560.
- Ryneerson G.A. and Smith C.T., 1940. Chromite deposits in the Seiad Quadrangle Siskiyou County, California. U. S. Dept. Interior Geol. Survey Bull., 922-J: 281-306.
- Sarıfakioğlu E., Özen H. and Winchester J.A., 2009. Whole rock and mineral chemistry of ultramafic-mafic cumulates from the Orhaneli (Bursa) Ophiolite, NW Anatolia. *Turk. J. Earth Sci.*, 18: 55-83.
- Satsukawa T., Griffin W.L., Piaolo S. and O'Reilly S.Y., 2015. Messengers from the deep: Fossil wadsleyite-chromite microstructures from the Mantle Transition Zone. *Sci. Rep.* 5: 16484. doi:10.1038/srep16484.
- Schmidt M.W., Gao C., Golubkova A., Rohrbach A. and Connolly J.A., 2014. Natural moissanite (SiC)-a low temperature mineral formed from highly fractionated ultra-reducing COH-fluids. *Progr. Earth Planet. Sci.*, 1 (1): 1-14.
- Sinton J., 1977. Equilibration history of the basal alpine-type peridotite, Red Mountain. *New Zealand J. Petrol.*, 18: 216-246.
- Tavlan M., Thorne R. and Herrington R.J., 2011. Uplift and laterization history of the Çaldag ophiolite in the context of Neo-Tethyan ophiolite obduction and uplift: implications for the Cenozoic weathering history of western Anatolia. *J. Geol. Soc. London*, 168: 927-940.
- Thayer T.P., 1969. Gravity differentiation and magmatic re-emplacment of podiform chromite deposits. In: H.D.B. Wilson (Ed.), *Magmatic ore deposits*. *Econ. Geol. Monogr.*, 4: 132-146.
- Tian Y.Z., Yang J.-S., Robinson P.T., Xiong F.H., Li Y., Zhang Z.M., Liu Z., Liu F. and Niu X.L., 2015. Diamond discovered from chromitites in the Sartohay ophiolite, Xinjiang Province, China. *Acta Geol. Sinica*, 89: 801-809.
- Trumbull R.B., Yang J.-S., Robinson P.T., Di Piero S., Vennemann T. and Wiedenbeck M., 2009. The carbon isotope composition of natural SiC (moissanite) from the Earth's mantle: new discoveries from ophiolites. *Lithos*, 113: 612-620.
- Ulmer G.C., 1969. Experimental investigations of chromite spinels (with discussion). In: H.D.B. Wilson (Ed.), *Magmatic ore deposits*. *Econ. Geol. Monogr.*, 4: 114-131.
- Ulmer G.C., Grandstaff D.E., Woermann E., Göbbels M., Schönitz M. and Woodland A.B., 1998. The redox stability of moissanite (SiC) compared with metal-metal oxide buffers at 1773 K and at pressures up to 90 kbar. *N. J. Miner. Abhand.*, 172 (2): 279-307.
- Uysal İ., Akmaz R.M., Kapsiotis A., Demir Y., Saka S., Avcı E. and Müller D., 2015. Genesis and geodynamic significance of chromitites from Orhaneli and Harmançk ophiolites (Bursa, NW Turkey) as evidenced by mineralogical and compositional data. *Ore Geol. Rev.*, 65: 26-41.
- Uysal İ., Dokuz A., Kapsiotis A., Kaliwoda M., Karsli O., Müller D. and Aydin F. 2017. Mineralogy and geochemistry of the Neo-Tethyan Orhaneli ultramafic suite, NW Turkey: Evidence for the initiation and evolution of magmatic processes in a developing crust-mantle boundary. *Geophys. Res. Abstr.*, Vol. 19, EGU2017-13753, 2017, EGU General Assembly 2017.
- Uysal İ., Ersoy E.Y., Kardlı O., Dilek Y., Sadıklar M.B., Ottley C.J., Tiepolo M. and Meisel T., 2012. Coexistence of abyssal and ultra-depleted SSZ type mantle peridotites in a Neo-Tethyan Ophiolite in SW Turkey: constraints from mineral composition, whole-rock geochemistry (major-trace-REE-PGE), and Re-Os isotope systematics. *Lithos*, 132-133: 50-69.

- Uysal İ., Şen D.A., Ersoy E.Y., Dilek Y., Saka S., Zaccarini F., Escayola M. and Karlı O., 2014. Geochemical make-up of oceanic peridotites from NW Turkey and the multi-stage melting history of the Tethyan upper mantle. *Miner. Petrol.*, 108: 49-69.
- Xiong Q., 2015. Shenglikou and Zedang peridotite massifs, Tibet (China): Upper mantle processes and geodynamic significance. PhD thesis, Macquarie Univ., Sydney, NSW, 268 pp.
- Xu X.Z., Yang J.-S., Chen S.Y., Fang Q.S., Bai W.J. and Ba D.Z., 2009. Unusual mantle mineral group from chromitite orebody Cr-11 in the Luobusa Ophiolite of the Yarlung-Zangbo Suture Zone, Tibet. *J. Earth Sci.*, 20 (2): 284-302.
- Xu X.Z., Yang J.-S., Robinson P.T., Xiong F.H., Ba D.Z. and Guo G.L., 2015. Origin of ultrahigh pressure and highly reduced minerals in podiform chromitites and associated mantle peridotites of the Luobusa ophiolite, Tibet. *Gondw. Res.*, 27 (2): 686-700.
- Yamamoto S., Komiya T., Hirose K. and Maruyama S., 2009. Coesite and clinopyroxene exsolution lamellae in chromites: *In-situ* ultrahigh-pressure evidence from podiform chromitites in the Luobusa ophiolite, southern Tibet. *Lithos*, 109: 314-322.
- Yamamoto S., Komiya T. and Maruyama S., 2015. Modification of the High-Pressure-Type chromites into the Low-Pressure-Type: Petrological investigation of the podiform chromitites in the Luobusa Ophiolite, Tibet. *Acta Geol. Sinica (English Ed.)*, 89 (suppl. 2): 104.
- Yang J.-S., Dobrzhinetskaya L., Bai W.-J., Fang Q.-S., Robinson P.T., Zhang J. and Green II H.W., 2007. Diamond- and coesite-bearing chromitites from the Luobusa ophiolite, Tibet. *Geology*, 35 (10): 875-878, doi: 10.1130/G23766A.1.
- Yang J.-S., Meng F.C., Xiang Z.X., Robinson P.T., Dilek Y., Makeyev A.B., Wirth R., Wiedenbeck M. and Cliff J., 2015a. Diamonds, native elements and metal alloys from chromitites of the Ray-Iz ophiolite of the Polar Urals: *Gondw. Res.*, 27: 459-485.
- Yang J.-S., Robinson P.T. and Dilek Y., 2014. Diamonds in ophiolites. *Elements*, 10: 127-130.
- Yang J.-S., Robinson P.T. and Dilek Y., 2015b. Diamond-bearing ophiolites and their geological occurrence. *Episodes J. Intern. Geosci.*, 38 (4): 344-364.
- Zhang P.-F., Zhou M.F., Su B.X., Uysal I., Robinson P.T., Avcı E. and He Y.S., 2017. Iron isotopic fractionation and origin of chromitites in the paleo-Moho transition zone of the Kop ophiolite, NE Turkey. *Lithos*, 268-271: 65-75.
- Zhou M.F., Robinson P.T. and Bai W.J., 1994. Formation of podiform chromitites by melt/rock interaction in the upper mantle. *Miner. Dep.*, 29: 98-101.

Received, August 25, 2017

Accepted, October 9, 2017